UNIVERSITAT POLITÈCNICA DE CATALUNYA
BARCELONATECH

MASTER THESIS

Experimental study of the propagation of acoustic waves by means of a Laser Doppler Vibrometer

Anna Argelagós

SUPERVISED BY

Ricard González-Cinca
Francesc Suñol

Universitat Politècnica de Catalunya
Master in Aerospace Science & Technology
April 2014

Experimental study of the propagation of acoustic waves by means of a Laser Doppler Vibrometer

BY

Anna Argelagós

DIPLOMA THESIS FOR DEGREE

Master in Aerospace Science and Technology

AT

Universitat Politècnica de Catalunya

SUPERVISED BY:

Ricard González-Cinca

Francesc Suñol

Department of Applied Physics (EETAC-UPC)

ABSTRACT

Propellant storage in space missions could be more efficient with the ability to control the bubbles within the storage tanks. One of the effective options is to control bubbles using acoustic fields.

The following work entails the study of the behaviour of a wall of a cubic test cell containing fluid media when subjected to acoustic fields of different parameters. These studies are characterized by the change in the wall displacement, using a Laser Doppler Vibrometer, a piezoelectric, a shaker and the acquisition instruments. Following these experiments, calculations are carried out to observe its displacements. These results are checked for reliability and repeatability using a shaker at low frequencies to confirm the correct performance of the Laser Doppler Vibrometer. A large part of this experiment, using the test cell, is carried out using different fluid media; Air, distilled water and a mix of both.

The results observed from the experimental study can be reviewed in three different parts. The first one, regarding the displacement, which is bigger in the face wall than in the back wall of the test cell and the maximum displacement is done above the focus of the vibration source. The second one, regarding the attenuation of the acoustic wave, it is observed that the attenuation coefficient is not constant along the test cell. The third one is with regards to the frequency applied in the acoustic field, where the resonant frequency of the test cell generates more displacement of the walls than the resonant frequency of the piezoelectric used.

The results obtained in this document are important for the future of long term storage of propellant in aerospace vehicles, especially in rigid tanks with a mixture liquid-gas submitted to vibrations. Also, they serve as an additional reference to the future work and development of space storage systems.

ACKNOWLEDGEMENTS

I would like to express my gratitude to my advisors, Dr. Ricard González-Cinca and Dr. Francesc Suñol, for their excellent guidance, care and patience throughout this Master Thesis. Besides my advisors, I am particularly grateful for the assistance given by Dr. José García, for his contribution to the resolution of the technical problems that appeared during the measurements of the experiment. Also, I would like to thank all the members of the research group at the *Microgravity Laboratory* of UPC. This research project would not have been possible without their help.

I would also like to express my gratitude to the members of the direction of EETAC, especially to Antonio M. Gálvez, Rafael Vidal, Francisco Javier Ozón and Neus Negre, who actively works with me. All their understanding and advice through this period have been a key point to the development of this master thesis. I also thank my workmate Ana Andújar for her constructive comments and warm encouragement.

My deepest appreciation goes to Brandon Savio Bradford. He has been my left hand, sometimes also the right, along this thesis, and without his support and persistent help, this thesis would not have materialized. I owe my deepest gratitude to him not only as a colleague, but also as a friend and, the most important of all, as a life partner.

Last but not the least, in fact for me the greatest pillar that holds me, special thanks to all my family for their unconditional faith in me. Your continuous and encouraging support is invaluable.

Table of Contents

List of Figures

List of tables

INTRODUCTION

Laser Doppler Vibrometry is a non-destructive and non-contact method useful in the testing of mechanical properties in a wall separating two media [1]. This is an experimental method to study how mechanical energy, when transferred to different media, affects the receiving surface. This experiment will utilize this LDV technology coupled with the use of *acoustic fields.* Acoustics is the study of mechanical waves in gases, liquids, and solids originated from a sound. The acoustic wave is generated by the propagation of a mechanical perturbation, which in turn generates an acoustic field within a closed structure.

Controlling bubbles within a fluid medium can help scientists improve the performance of many aerospace systems. Research has been done over the years to try to improve system applications such as fuel storage for rockets, for the continuity of human life in a space environment to be possible. One possibility to control bubble flow is to use acoustic fields. Nevertheless, these acoustic fields have effects on the surrounding environment as well. This document explains the experimental study that was carried out in order to analyse, using Laser technology, the effects of acoustic fields of various magnitudes, on a surface which contains a fluid media within it.

To address the requirement of the effect of acoustic fields on surfaces containing fluids, research has to be done in this field of aerospace technology. This master thesis presents an experimental study which involves the transfer of mechanical energy from an acoustic field to the aluminium wall of an object under different conditions of fluid media.

The goal of this project is to experimentally study the various effects that acoustic fields of varying parameters have on a defined test cell containing fluid media of different volumes, using *Laser Doppler Vibrometry*, in order to use this data in future scientific research involving acoustic behaviour on a rigid body containing fluids.

The outline of the present work is divided into 4 chapters. In Chapter 1, the introduction to the topic and the different concepts applied are explained. This chapter is divided in two main parts. The first one related to *the acoustic field*, its principle and general applications. The second one is related with the principle of *a Laser Doppler Vibrometer (LDV)*. The relation between both these parts is that an LDV can measure the displacement created on a surface due to the propagation of an acoustic wave, which is the main purpose of this work.

In Chapter 2, the experiment is outlined, starting with the different devices used, and followed by the experimental set-up. In this case, there are two experimental set-ups which belong to two similar studies; one is related with a *shaker,* for low frequencies, and the second one uses a *test cell*, where when connected to a piezoelectric, an acoustic field is generated and passed through it. Due to the similarity of both experiments, after the experimental set-up, the experimental procedure and analysis of both cases are explained.

In Chapter 3, the results obtained from the experiments are presented and discussed. In this chapter, the information is divided into two main parts. The first part regards the study at low frequencies, corresponding to the shaker measurements. The second part regards high frequencies, corresponding to test cell measurements.

Finally, in Chapter 4, all the main results obtained along the course of the experiments are reviewed and summed up in the conclusions. Furthermore, future lines of investigation regarding an acoustic field, and the use of an LDV to help understand its effects are outlined.

Chapter 1

ACOUSTIC FIELDS AND THE LDV

This chapter will outline the working principles of both, the acoustic field and the LDV. As can be seen later in this document, these two phenomena will work in cohesion with each other to complete the experiment.

1.1. Acoustic Field

Acoustics is known as the study of mechanical waves in gases, liquids, and solids originated from a sound. In this definition, the study of vibrations, ultrasound and infrasound are explained, which are named differently depending on their characteristics. The acoustic wave is generated by the propagation of a mechanical perturbation, which in turn generates an acoustic field within a closed structure.

This section will explain, in detail, the definition of an acoustic wave, Bjerknes forces, and finally end with some applications of acoustic fields.

1.1.1. Acoustic Wave

As mentioned before, an acoustic wave is an oscillation of pressure, displacement and density which propagates through a solid, liquid, or gas due to a mechanical perturbation. This wave can be defined by its wavelength, its frequency and its amplitude of propagation.

When the oscillation of an acoustic wave stays in the same position, it is called *stationary wave*, because it does not transport mass. In a contrary case, the wave is called a *progressive wave*. The variation of displacement with time that is followed by the acoustic wave is defined as:

$$s(x,t) = s_0 \sin\ (kx - \omega t) \tag{1.1}$$

The displacement is done along the direction of the movement of the wave and produces a change in the acoustic pressure and density of the media. The acoustic pressure wave is phased at 90º with respect to the acoustic displacement wave. For that reason, the acoustic pressure obtained by an acoustic wave is defined as:

$$p = p_0 \sin\left(kx - \omega t - \frac{\pi}{2}\right) \quad \textbf{(1.2)}$$

Where 'p' is the change in pressure with respect to the equilibrium position and 'p_0' is the maximum value of this change. This amplitude of pressure is related with the maximum amplitude of displacement 's_0' by the density 'ρ' and the propagation velocity 'v'.

$$p_0 = \rho \omega v s_0 \quad \textbf{(1.3)}$$

1.1.2. Bjerknes Forces

Bjerknes proposed some forces based on the law of buoyancy for the bubble, which can be applied to the acoustic field inside a closed environment. The proposal states that the buoyancy is equal to the product of the acceleration of the translator motion, multiplied by the mass of water inside the closed structure [2]. This is known as the Bjerknes force on an air bubble, which is composed of by the volume of the bubble '$V(t)$' and the pressure gradient of the field applied '$\nabla p_a(r,t)$'. Hence, the Bjerknes force is commonly expressed as:

$$F_B = -\langle V(t) \nabla p_a(r,t) \rangle \quad \textbf{(1.4)}$$

However, when a stationary acoustic field is applied, this primary Bjerknes force can produce two opposite phenomena on the bubble; the first one being the attraction of the bubble towards the pressure antinode and the second one, repulsion. The bubble will be attracted toward the pressure antinode when it is driven above its natural resonance frequency. Otherwise, the bubble will move towards the pressure node. Also, the secondary Bjerknes forces, which takes effect between two nearby bubbles, can also be influenced by some boundary conditions of neighbouring oscillating bubbles [3][6].

1.1.3. Applications

The amount of fields where acoustics can be applied is quite extended. Some examples include location purposes, as SONAR in submarines, or medical examinations, to get images of a fetus from a mother's womb.

Regarding the study of fluids, which has become important in recent years owing to the increasing number of applications in this field, research and experimentation has been made. One example is the work done by Xi et al [4] who studied the interactions between bubbles and a surface experimentally and analytically. From this work they observed that the bubble trajectory depends on the acoustic pressure amplitude and the initial bubble size. Furthermore [3], they

continued to study a multi-bubble transport method by using an acoustic standing wave, from where, they observed the influence of primary Bjerknes force, secondary Bjerknes force, and buoyancy force on the bubble translation depends on the position of the target bubble in the acoustic field.

Related with boiling, Douglas et al. [5] studied that enhancement of a bubble detachment process also suppresses the transition to film boiling. In microgravity conditions, some experiments have been done, such as one from Sitter et al. [6], who study the interaction between an acoustic field and a pool boiling system in normal gravity and microgravity, from which they observed that the acoustic force on a bubble plays the role of buoyancy in microgravity.

Another interesting application and investigation done with both fields, fluids and acoustics, is the one from Asaki et al [7], where they trap a 5 mm air bubble, approximately, into a concrete location, within a steady wave, creating a stable levitation. Then, using an LDV, they measure the shape oscillations of the bubble in the levitator. This is an example of how two different areas, such as, in this case, acoustics and an LDV, can be a perfect conjunction for an experiment of this kind. In this direction, within the next sections, the principle of the LDV is explained.

1.2. Laser Doppler Vibrometer (LDV)

A Laser Doppler Vibrometer (LDV) has been developed with the aim of measuring the velocity and displacement of moving surfaces using a non-destructive and non-contacting method. Therefore, it has become a very useful laboratory tool for this purpose: detects the vibrations of the moving surface of an object. As explained in section 1.1, the wave of an acoustic field generates a vibration in the surfaces to which it is applied. This vibration can be analysed using an LDV device. In this section, the principle of the LDV and some applications are explained.

1.2.1. Principle

An LDV is an instrument for non-contact measurement of surface vibrations based on laser interferometry [8]. Its technology is based on the Doppler effect, in which it senses the frequency shift of back scattered light from a moving surface [9]. In other words, the light scattered from a moving object is frequency shifted with respect to the incident light [10] to calculate the velocity of the displacement of the moving surface.

The Doppler effect is the apparent change in the frequency of a wave caused by the relative motion between the source of the wave and the observer. This phenomenon is observable when an ambulance passes close with its siren blaring. At the beginning, the listener can hear the high pitched siren as it approaches, and as it is moving away, the siren pitch changes the sound and it starts to lower. As can be observed in Figure 1.1, this phenomenon is caused due to the changing distance between the source of the waves and the observer.

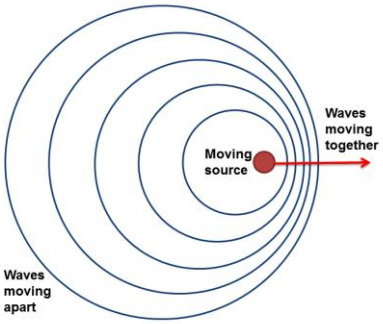

Figure 1.1 The Doppler effect.

To be able to determine the velocity of an object, the frequency shift has to be measured at a known wavelength. This is done in the LDV by using a laser interferometer [9].

The interferometer compares characteristics of an object beam with that of an internal reference beam which, in the case of an LDV, are the frequency and the phase. The frequency difference is proportional to the instantaneous velocity and the phase difference is proportional to the instantaneous position of the object [8]. The optical interference can be observed when two coherent light beams are made to coincide [8]. More details of the optical configuration of the interferometer from the LDV used are explained in section 2.1.3.

1.2.2. Applications

The LDV technology is widely used for different applications and fields. The primary applications of the LDV have been in the metal industries. One example is in the steel industry, where the biggest application is for measuring the length of hot steel for cut-to-length applications and the quality assurance on bar and structural steel rolling mills [10]. Nevertheless, nowadays the use of this device has been extended in other fields, such as scientific, medical, security and art.

One important application is the aerospace and automotive field. LDV technology is used in order to check structural dynamics, quantifications of vibrations and fatigue of the materials and the components of the different vehicles. These tests are also applied on architecture, where the LDV is used for a structural analysis of the buildings, bridges and roads.

Another application is related with acoustics; for example, in speaker design and musical instruments, which analyse the performance of new devices. There is a new application in the field of music and art, from the importance to correct and determine the state of conservation of artworks. This is an example of the work of Esposito (see [11] and [12]) and also Collini et al [13], where they propose this technology to analyse the preservation state of art, being helped by an acoustic sound (speakers).

Regarding the mechatronics field, due to the presence of small components, which requires precision analysis, the LDV is a perfect in situ diagnostic method for structural health monitoring of Plasma Facing Components, to identify specific damage mechanisms including cracking and erosion, especially in elevated temperatures and also in the presence of high magnetic fields and neutrons. This example is of the work of Luna Innovations (see [14]).

Chapter 2

EXPERIMENTS USING AN LDV

As introduced in Chapter 3, acoustics is the study of a wave, which is propagated along an environment. This wave generates a movement depending on the environment in which is performed. If this wave is generated inside a test cell, its walls, as well as its contents, are going to be subjected to a vibrating movement.

An LDV is a device which computes the velocity and displacement of a vibrating object at the level of μm, which cannot be recorded or analysed by a high speed camera. For that reason, an LDV is the best tool to measure the vibrating movement of the walls of an object, on which vibrations are generated due to an acoustic field.

Nevertheless, before measuring the vibrating movement of the vibrating object due to an acoustic field, it is necessary to check the performance of the LDV with an object whose displacement can be recorded by a high speed camera. A shaker has been used at low frequencies to this purpose. Following this, a quite similar experiment has been done using a test cell at high frequencies. Therefore, in this chapter, the different devices and equipment used for both studies, followed by the experimental set-ups are introduced. Furthermore, the experimental procedure for the experiments and the experimental analysis in each experiment, with the different cases are studied.

2.1. Experimental equipment

2.1.1. Shaker

The V200 Series electro-dynamic vibration generators are miniature units designed to reproduce a vibration environment under laboratory conditions. This device performs an oscillatory movement which can measure and calculate its displacement. The useful Frequency Range is 5-13000 Hz [15]. The reference object used is a screw of 3 grams in weight, to be able to record the movement using the camera and measure the velocity using the LDV. In Figure 2.1, the shaker used with a Laser beam focused on the screw head is shown.

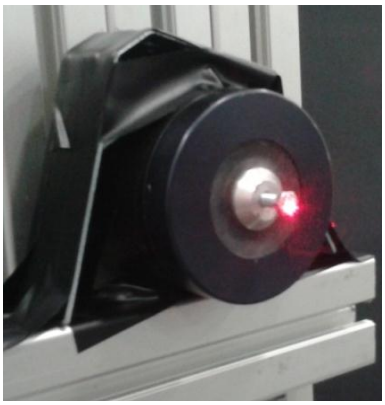

Figure 2.1 Shaker with a Laser beam focused on the screw head.

2.1.2. Test Cell

The inner dimensions of the test cell used are 9x9x9cm, wherein the water is filled. The walls are 11x8cm. The Test Cell is connected to a Piezoelectric with epoxy glue. The Piezoelectric is the device which generates the acoustic field inside the test cell and it has a radial resonance frequency of 53 kHz, and a lateral resonance frequency of 680-750 kHz. A picture of the Test Cell is shown in Figure 2.2.

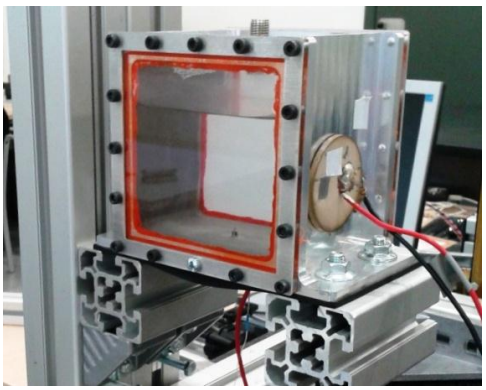

Figure 2.2 Test cell.

2.1.3. Laser Doppler Vibrometer

The Laser Doppler Vibrometer is used to measure the displacement of the walls of the test cell, generated by the piezoelectric and the screw head from the shaker. The model used in this experiment is a Polytec Laser Doppler Vibrometer which consists of a Controller OFV-3001 and a Sensor Head OFV-303.

The sensor head emits a beam of Helium-Neon (He-Ne) laser, focused on the object of study. The beam is then scattered back from the surface and coupled back into the interferometer, on the sensor head [8]. The laser in the sensor head needs a time period of 20 minutes to achieve certain optimum stability, and to make the first

measurements in thermal equilibrium with the LDV surroundings [8]. A schematic connection of signals in the sensor heads are shown in Figure 2.3.

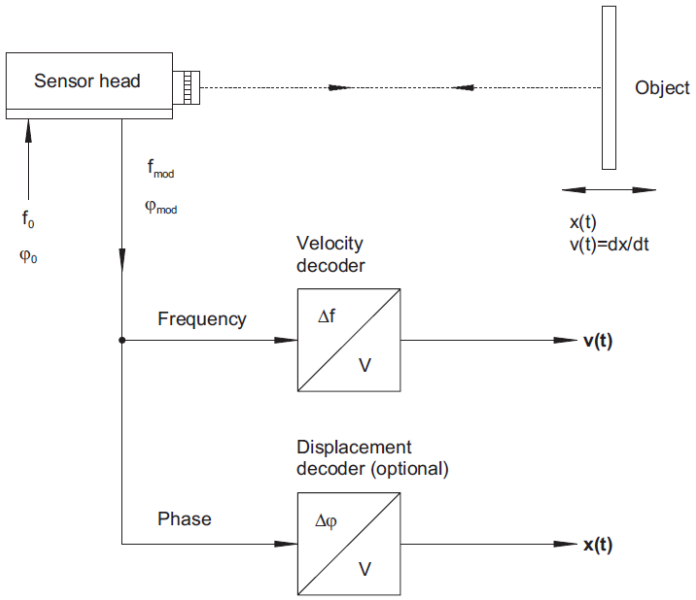

Figure 2.3 Signals from the laser beam emitted and received at the sensor head OFV-303 [8].

In this system, velocity and displacement measurements are carried out by the LDV using a modified Mach-Zehnder interferometer; a device used to determine the relative variations between two parallel beams split from a single source. The He-Ne laser beam is send to the first beam splitter, BS1, which splits the beam into two different paths: the *object beam* and the *reference beam* [8]. The optical configuration in the sensor head is shown in Figure 2.4.

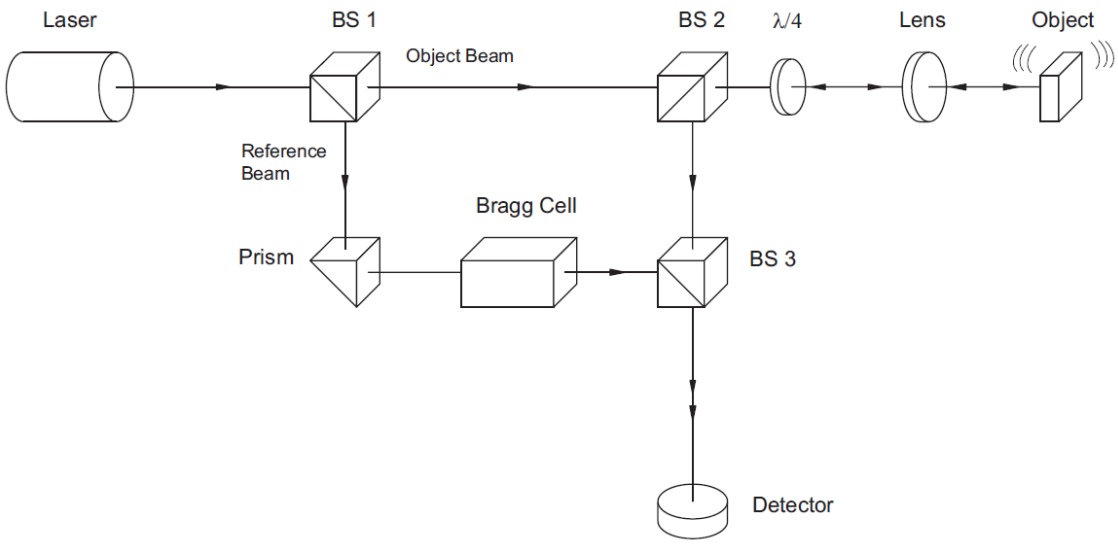

Figure 2.4 Optical configuration of the interferometer in the sensor head OFV-303 [8].

As can be seen in Figure 2.4, along one of the paths, called the object beam, the beam passes through a second beam splitter, BS2, and then, towards the λ/4 plate, to be focused by the lens on the object, and further scattered back from there. The beam splitter BS2 also redirects the object beam to the beam splitter, BS3, with the help of the λ/4 plate.

The second path of the originally split object beam, called the reference beam, is redirected through a prism and send to the Bragg cell, to give information about the direction of the velocity of the object that is being measured. Furthermore, this Bragg cell will also shift the frequency of the laser beam when the object is moving towards the interferometer, due to Doppler effect [9]. On the other side, the Bragg cell also receives the redirected beam from the splitter BS3 which comes from the beam splitter BS2. Since these two beams are symmetrical, the optical path difference between the object beam and the reference beam vanish within the interferometer. The resulting path difference is equal to twice the distance between the beam splitter BS2 and the object (because of the distance travelled by the beam).

After this, the beam that passes through the Bragg cell, is sent to beam splitter BS3, to be redirected to reach the detector. The resulting interference signal of the object beam and reference beam is converted into an electrical signal in the detector and subsequently decoded in the controller [8].

On another side, the main function of the controller is to use the signal from the sensor head to process it and decode it. The controller takes the signal from the interferometer and it demodulates them. The information extracted from the signal can be divided in two different parts which give different information. The first one, proportional to the instantaneous velocity, belongs to the frequency of the signal. The second one, proportional to the displacement of the object, belongs to the phase of the signal. The information is available at the front of the controller as an analogue voltage which can be processed externally with an oscilloscope [8].

The controller is operated via a menu on the display of the controller. Mean, velocity decoder, velocity range and velocity filter can be selected according to the most appropriate situation of the object under study. This menu also has secondary functions such as filters to improve and display different settings, in order to be more user friendly [8].

2.1.4. Structure

The structure has been designed to have more accurate data, to mitigate the error, to reduce the fluctuations of the data obtained from the LDV and to have repeatability in the measurements. The structure also reduces the noisy signal from the LDV considerably. It is divided into three parts; the base, the support for the sensor head of the LDV and the vibrating object support which, in this case, is the test cell and the shaker. Figure 2.5 shows the different parts of the structure.

The base is the lower part of the structure which connects and gives stability to the support of the laser with the support of the object to be analysed. This part of the structure ensures the distance between the object and the LDV, which has to be at least 45 cm.

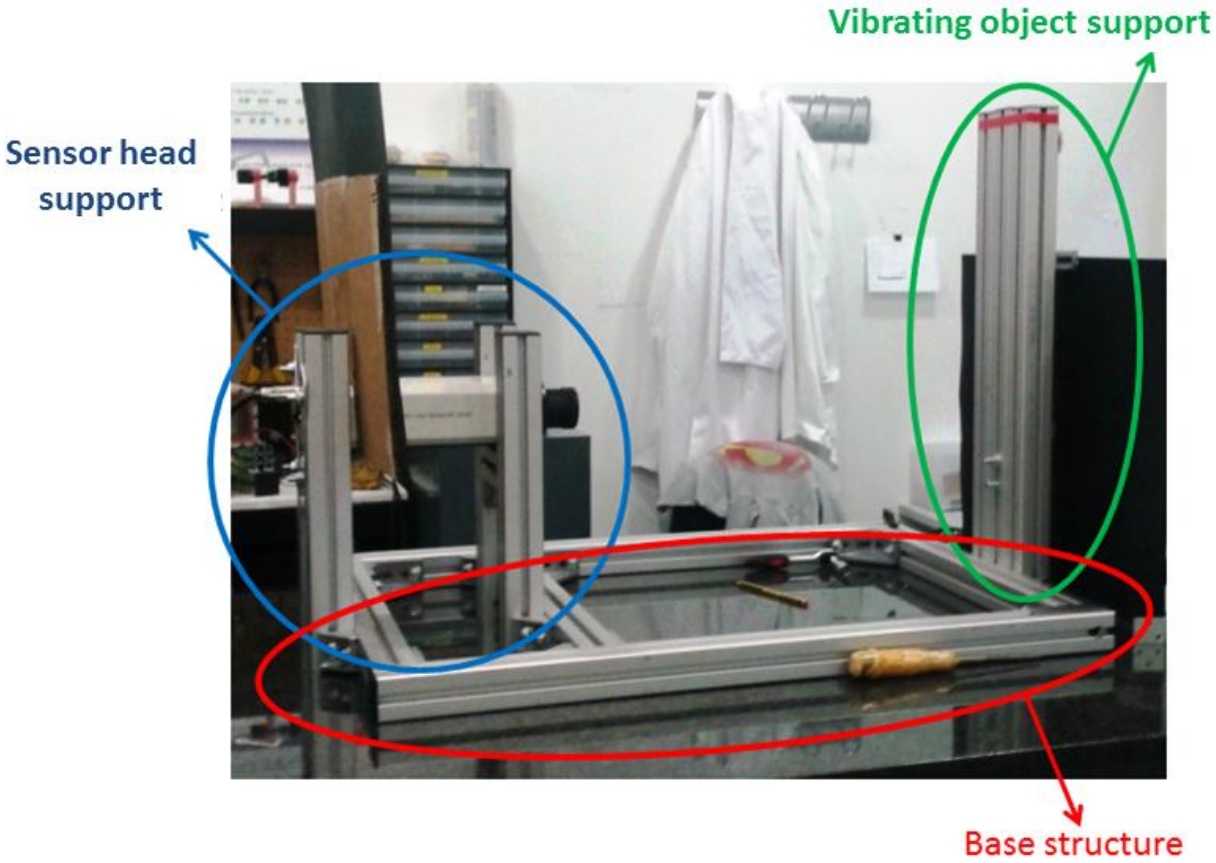

Figure 2.5 Structure build for the experiment.

The vibrating object support is made up of three columns to have more stability. It is attached to the columns as is shown in Figure 2.6. The columns are movable to right and left and, in the case of the test cell, it can move up and down.

Figure 2.6 Vibrating object support.

The support of the sensor head is shown in Figure 2.7 and is constructed with 4 columns of *Bosch Aluminum profiles* attached to the base of the structure and further, with 2 transversal tubes. This part of the structure was made in order to arrest any movement in the measurements from the sensor head of the LDV.

Figure 2.7 Sensor head support with Bosch tubes.

2.1.5. Camera and backlight

The camera used is a High Speed camera model Redlake Motion – XTRA HG-SE. The camera records 4 seconds videos at a frequency of 1000 frames/second. In order to be able to observe the videos from the camera, a backlight is also used in the experiment. This backlight is composed by an array of LEDs. In Figure 2.8, these devices with the shaker used in the experiment for the experimental set-up are shown.

2.1.6. Data acquisition instrument: Oscilloscope

In order to read the information obtained from the LDV, a Tektronix TDS 2022B oscilloscope is used. This oscilloscope is composed of by 2 channels.

2.1.7. Input control devices: Waveform generator and Amplifier

Two input control devices are used in order to apply a voltage to the vibration object. The first one is a waveform generator, which is a model Agilent 33210A with 10 MHz function/arbitrary. The second one is a Falco systems amplifier, DC – 5 MHz High Voltage Amplifier WMA-300 model, which takes the voltage generates by the waveform generator and amplifies it.

2.2. Experimental set-ups

In order to know more about the performance and functionality of the Laser, a study of the measurements at low frequencies from a shaker has been done. The objective of this study is to check the good performance of the laser. After that, the measurements with the laser have been done at high frequencies with the test cell. For that reason, the experimental set-up of both experiments, low frequencies and high frequencies, is very similar. The only difference is that the shaker base is not meant to be movable, while that of the test cell is. Also, in the shaker study, some videos are taken, to be compared with the data obtained from the LDV. Despite those differences being minimal, in this subsection, the experimental set-up is divided in two parts: the shaker set-up and the test cell set-up.

2.2.1. Low Frequencies vibration: Shaker

The experiment consists of the shaker described in section 2.1.1, connected to a waveform generator which, at the same time, is connected to an amplifier (see section 2.1.7). They generate the voltage needed in order to make the reference object of the shaker move. The movement is recorded by a Redlake high speed camera. In order to maximize the image contrast, an array of LEDs is added to the background. As a result of the light, the images recorded have a white background that contrasts with the black of the shaker and its reference object. Figure 2.8 presents the elements of the shaker, the high speed camera and the backlight from the experimental set-up. For more information about the camera and the backlight see section 2.1.5.

Figure 2.8 Shaker, high speed camera and backlight.

On the other hand, the measurement of the velocity on the head of the shaker screw has been carried out using a Polytec single point LDV, explained in detail in section 2.1.3. The laser beam from the sensor head of the LDV is focused on the head of the screw of the shaker. The reflected signal comes back to the sensor head of the LDV to be processed and converted into a voltage, displayed on a connected Tektronix oscilloscope (see section 2.1.6). Hence, this oscilloscope gives the information from the velocity of the object in volts. Figure 2.9 shows the experimental set-up described for the shaker study.

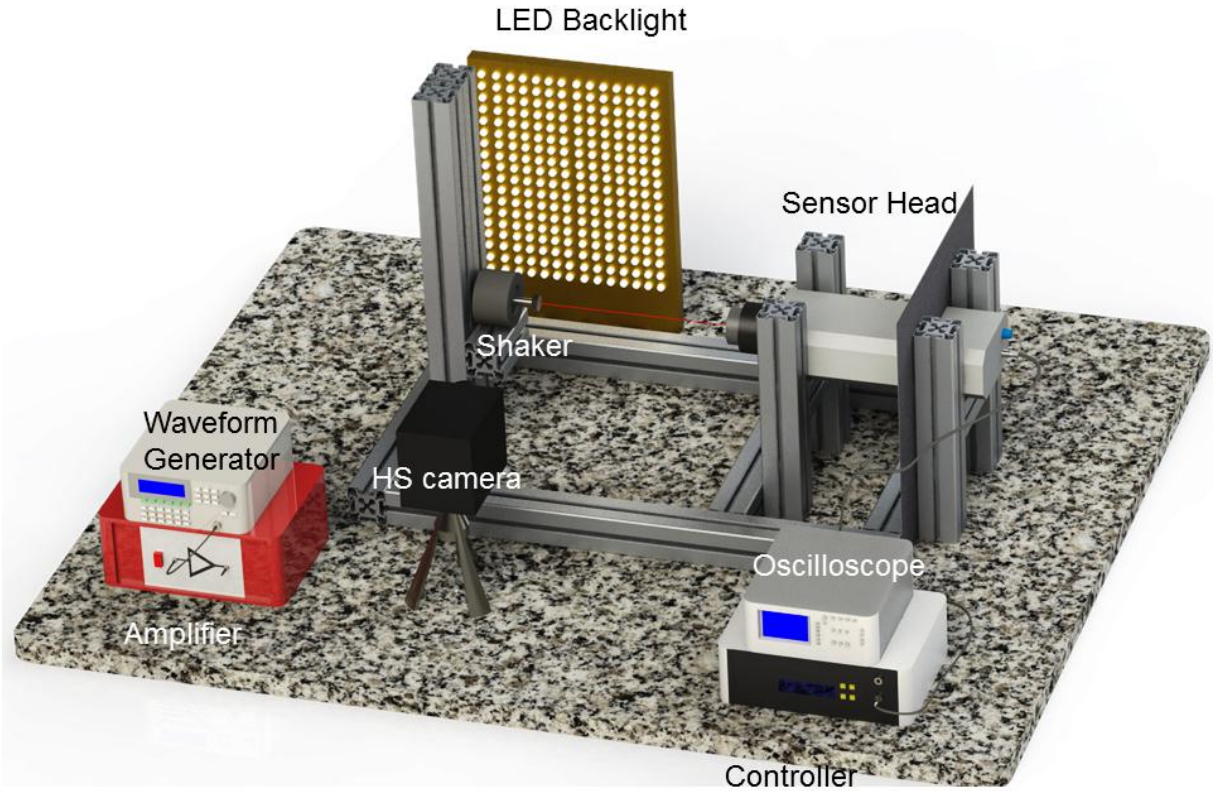

Figure 2.9 Experimental set-up of the shaker study.

2.2.2. High Frequencies vibration: Test cell

The experimental set-up of the test cell is similar to the set-up described in the section above (see section 2.2.1). Their two differences being, firstly the measurement of the movement from the surface of the walls of the test cell, instead of a reference object (shaker screw), and secondly, the video recorder set-up is not applied, due to walls generating movements so small that it is unable to be recorded.

The test cell, explained in detailed in section 2.1.2, is connected to a Piezoelectric which generates an acoustic field inside of it. To apply the acoustic field, a waveform generator is connected to an amplifier (see section 2.1.7) and then connected to the piezoelectric, which is then attached to the outer side wall of the test cell. From the moment the waveform generator and the amplifier are switched on with the desired frequency and voltage, the acoustic fields start to play.

The measurement of movement of the walls has been carried out using the same set-up of the LDV used in the shaker (see section 2.1.3) connected to a Tektronix oscilloscope (see section 2.1.6). In that case, the laser beam is focused on the wall of the Test Cell. Figure 2.10 shows the experimental set-up of the Test Cell.

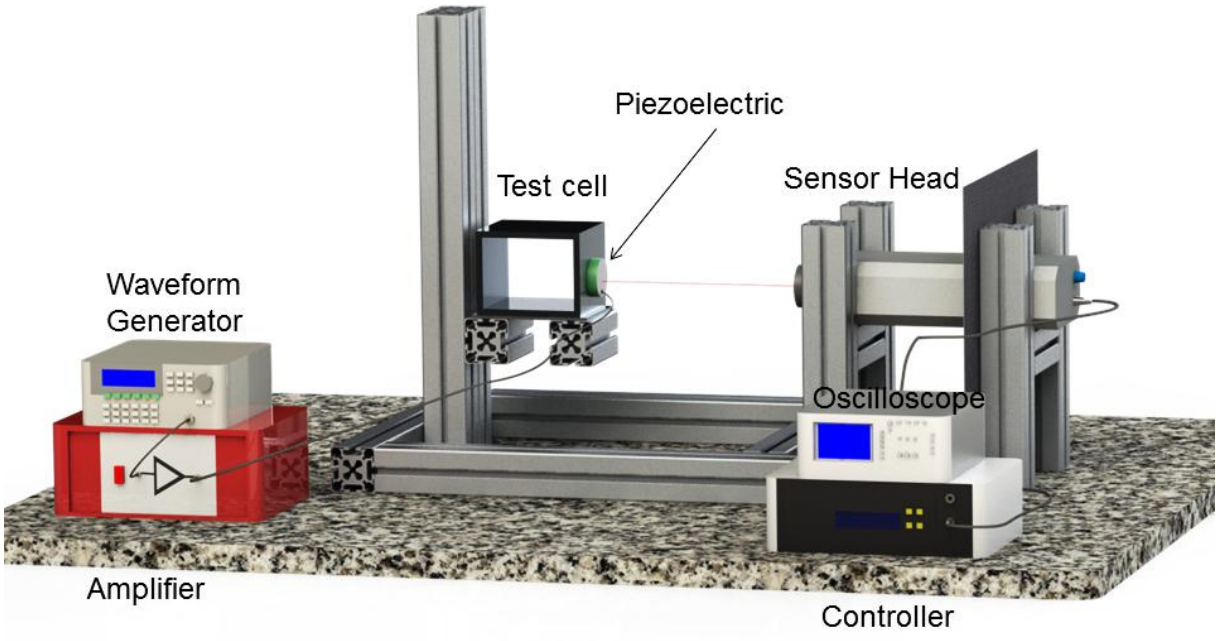

Figure 2.10 Experimental set-up of the test cell study.

2.3. Experimental Procedure

As mentioned in section 2.1, the study of the shaker has been performed in order to check the good procedure of the performance of the LDV. For that reason, as observed in the experimental set-up, the experimental procedure is also quite similar between both studies. Besides that, the conditions from both devices are

different. In this section the procedure used in the experimental studies and the conditions applied in both cases are introduced.

2.3.1. Procedure and conditions of the shaker

The study of the shaker has two different parts. The first part is related with the image acquisition of the screw of the shaker and the second part is related to the data acquisition from the LDV. The conditions measured from the shaker of both parts are the same, in order to be able to compare them. Those conditions measured in the shaker are shown in Table 1. They have been chosen in order to be able to record the movement using a Redlake high speed camera (see section 2.1.5).

Table 1 Frequencies and Amplitudes used in the study of the shaker.

Frequency (Hz)	**25**			**50**			**75**			**100**			**125**			**150**		
Amplitude (V)	1	3	6	1	3	6	1	3	6	1	3	6	1	3	6	1	3	6

First, the waveform generator and the amplifier are switched on, to generate the vibrational movement of the shaker screw. The frequency and amplitude to be studied is selected on the display of the waveform generator. With the high speed camera and the backlight on, a video of 4 seconds (with a frequency of 1000 frames per second acquisition) is taken for each case. From the frames of the video, images are extracted in order to analyse them. The analysis of these frames is explained in detailed in section 2.3.1.

The processes of the LDV and of the shaker, which is connected to the waveform generator and the amplifier, are quite similar; they are switched on, with the required frequency and amplitude selected. The controller has to be switched on 20 minutes before starting the measurements, in order to be thermally stabilized with the environment. With the velocity range and velocity filter appropriated for the measurements, the sensor head is switched on, and a laser beam is focused on the shaker. Furthermore, the laser beam has to be focused on the surface of the object, until achieving a fully lighted signal on the display of the sensor head. This signal corresponds to the signal-to-noise ratio, which is maximum if the signal level is full [8]. The data of the velocity is displayed on the oscilloscope in voltage, which is written down in *Microsoft Excel* with all the details of the measurements (frequency, amplitude).

For measurements in other conditions, the frequency and amplitude from the waveform generator, the procedure of both data acquisitions, video and LDV have to be changed. The only difference is that once the controller has been switched on for the first time, and after the 20 minutes of warming has been achieved, the next measurements can be performed automatically after the first one.

2.3.2. Procedure and conditions of the Test Cell

The procedure to take the measurements of the velocity of the walls of the test cell is very similar to the procedure used in the shaker. The only difference being that no video has been recorded for the test cell, and therefore, the image acquisition procedure has not being performed. Only the LDV movement measurement has been performed. This is because the small displacement of the walls could not be captured by the camera. Apart from this, the conditions of the test cell are different.

Tests have been performed at 53 kHz, at the radial resonance frequency of the piezoelectric, for the two sides of the Test Cell; the face, to which the piezoelectric is attached, and the back. The amplitudes applied from the waveform generator have been from 1V to 6V. The conditions inside the test cell performance are three: full of distilled water, half full of distilled water with half full of air, and empty of distilled water and hence full of air. These different conditions are summarized in Table 2.

Table 2 Conditions used in the study of the shaker.

Frequency (kHz)	**53**					
Amplitude (V)	1	2	3	4	5	6
Inside Conditions	Empty of water		Half of water		Full of water	
Side	Face			Back		

The different conditions measured have been applied and repeated across both walls of the test cell, in order to have a map of the displacement on the two sides (face wall, where the piezoelectric is located, and back wall on the other side). A grid has been marked on both walls. The aim of this grid is to measure inside the square for the different cells and therefore, having all the conditions measured inside every point of the grid. Figure 2.11 shows the grid and the nomenclature used to do the measurements.

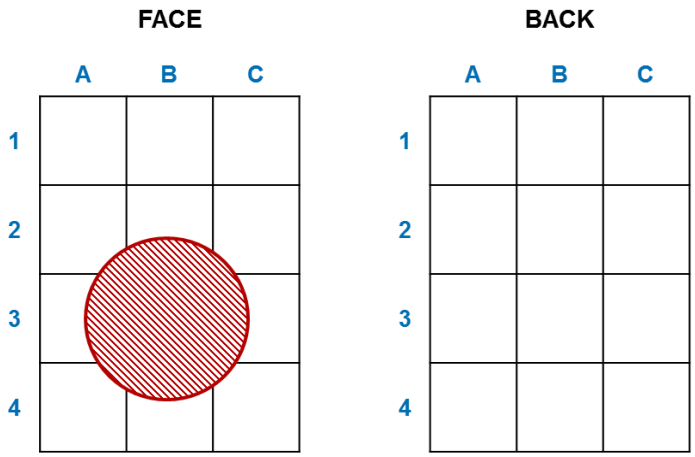

Figure 2.11 Grid used in the test cell measurements.

2.4. Analysis

2.4.1. Video processing

Each video recorded during the experiment was stored on a computer. There, all the frames of each video were also ripped and stored. From the frames of the video files, the images of the vibrating object (the shaker screw) are extracted in order to be analysed with ImageJ, to find the maximum displacement, in mm, of the vibrating screw between the minimum and maximum point of the movement. To extract the distance in mm, ImageJ allows you to change the scale from pixels to mm. Figure 2.12 shows the visible displacement of the head of the shaker in Image J and how it is measured.

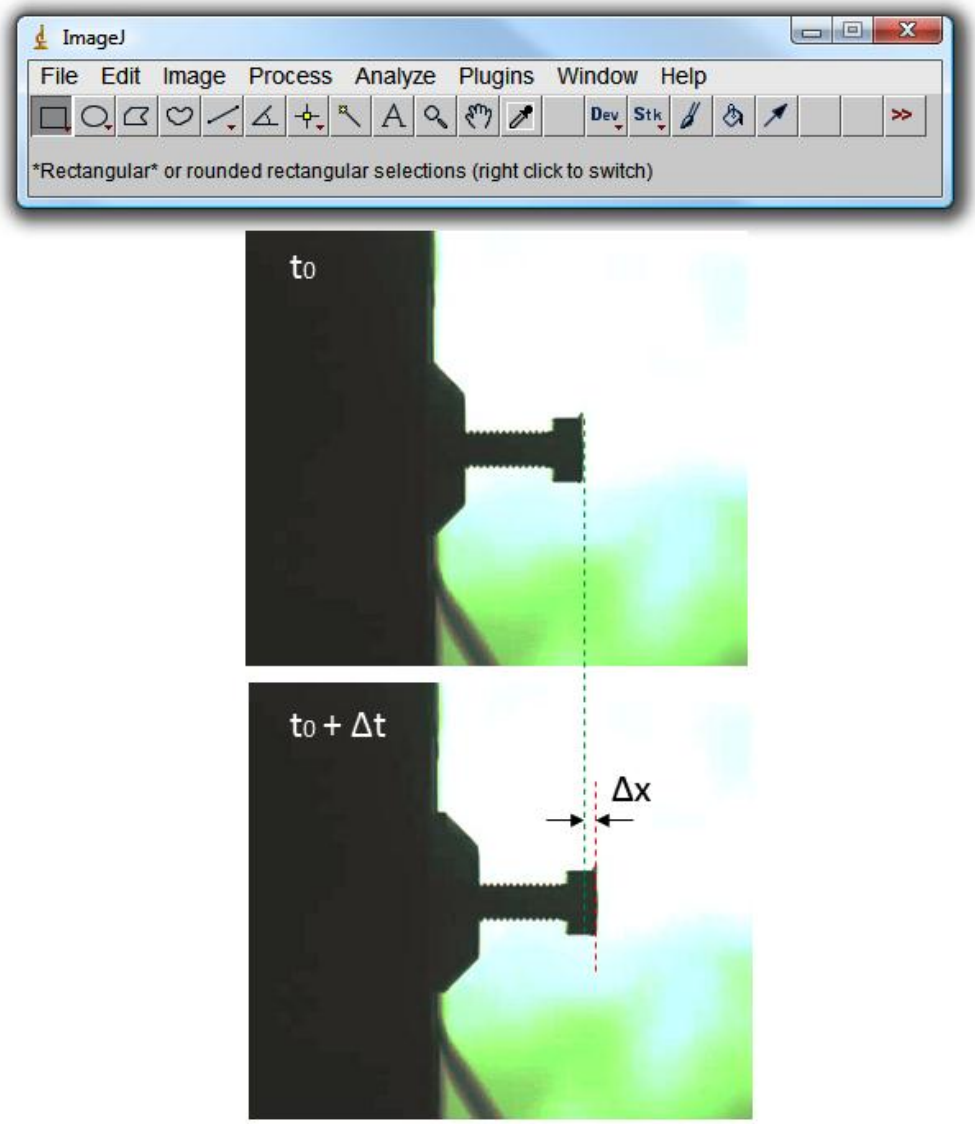

Figure 2.12 Visible displacement between the heads of the shaker screw in ImageJ.

2.4.2. Velocity measurement

The LDV can provide information related to the velocity and the displacement of the object under investigation independently [8]. Despite this, the measurements taken in this experimental study are only with regards to the velocity of the different surfaces.

As mentioned before in section 2.2.1, the LDV sends information about the velocity in terms of voltage to the oscilloscope, which displays it. This information can be converted to velocity (mm/s), with the velocity range applied at every case, and afterward, to displacement according to:

$$V = 2\pi f \hat{x} \tag{2.1}$$

Where, 'V' is the velocity once converted to mm/s, 'f' is the frequency from the vibrating object generated by a waveform generator, and '$\hat{x}$' is the surface displacement.

In Figure 2.13, the display of the oscilloscope used is shown. From the signal received, the voltage *peak-to-peak* was taken. For example, in this case (movement of the shaker at 150Hz and 6V) the value obtained from the LDV is 3,92V. This measure has been converted to velocity, with the velocity range used and selected in the controller as 125mm/s/V. Then, applying Equation 1, and using the frequency of the object, the displacement is calculated, which in this case is 0,52mm.

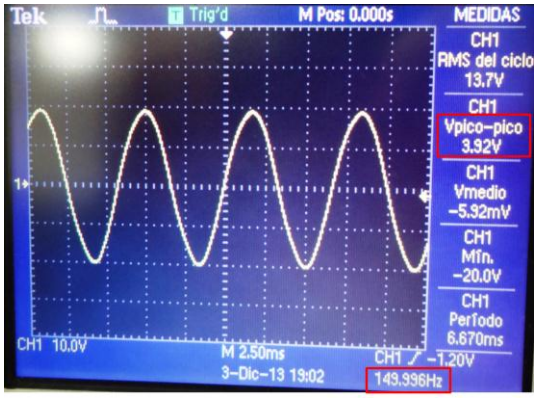

Figure 2.13 Tektronix TDS 2022B oscilloscope display response from the LDV of the shaker head at 150Hz and 6V showing measurements.

In order to be able to compute all the measurements and convert them from voltage to velocity-displacement, the conversion has been automated with Microsoft Excel. All the results of the measurements of, both, the shaker and the test cell are introduced in Chapter 3.

Chapter 3

EXPERIMENTAL RESULTS

This chapter details the experimental results obtained from both studies described in Chapter 2. The purpose of the study of the shaker, which was performed at low frequencies, is to check that the procedure of data acquisition from the LDV can be considered as both quantitative and qualitative, and therefore reliable.

Once this study has been performed, a study of high frequencies with the test cell, the object which generated vibrations due to an acoustic field applied on it, has also been done. The following sections will outline the studies of both, the shaker and the test cell, performed in the laboratory.

3.1. Low frequencies: study of the Shaker

As mentioned in the experimental set-up (see section 2.1.5) the shaker study has two parts, intended to be compared between them; the recorded videos and the LDV data. The results obtained from the different videos can be observed in Table 3, where the values from the recorded videos are detailed after having been processed.

Once the analysis of the videos (see section 2.3.1) has been performed for each case, detailed in Table 1 from section 2.3.1, the displacement, in mm, obtained for the head of the shaker is shown in Table 3.

Table 3 Displacement from the different videos at different frequencies and amplitudes.

Frequency (Hz)	Amplitude (V)	Displacement (mm)
25	**1**	0,243 (± 0,09)
	3	0,445 (± 0,09)
	6	0,879 (± 0,09)
50	**1**	0,232 (± 0,09)
	3	0,650 (± 0,09)
	6	0,991 (± 0,09)
75	**1**	0,216 (± 0,09)
	3	0,771 (± 0,09)
	6	1,219 (± 0,09)
100	**1**	0,232 (± 0,09)
	3	0,782 (± 0,09)
	6	1,181 (± 0,09)

125	**1**	0,223 (± 0,09)
	3	0,444 (± 0,09)
	6	0,671 (± 0,09)
150	**1**	0,108 (± 0,09)
	3	0,344 (± 0,09)
	6	0,447 (± 0,09)

In Table 3, it can be observed that as the amplitude is increased, the displacement of the shaker increases. Furthermore, at around 100 Hz, the displacement is much higher than at any other conditions. This is due to the performance of the shaker, which has a higher displacement around this frequency [15].

On another hand, using the same frequencies and amplitudes, the LDV part of this experiment has been carried out 5 times, spread out along time and, after analysing all the measurements, Table 4 has been obtained. In Table 4, what is observed is the average displacement between these 5 different measurements of each condition.

Table 4 Average displacement in mm from oscilloscope data.

Frequency (Hz)	Amplitude (V)	Average displacement (mm)
25	**1**	0,150 (± 0,004)
	3	0,552 (± 0,006)
	6	1,225 (± 0,034)
50	**1**	0,159 (± 0,003)
	3	0,562 (± 0,019)
	6	1,082 (± 0,011)
75	**1**	0,173 (± 0,003)
	3	0,744 (± 0,009)
	6	1,257 (± 0,018)
100	**1**	0,210 (± 0,004)
	3	0,774 (± 0,007)
	6	1,281 (± 0,041)
125	**1**	0,146 (± 0,002)
	3	0,504 (± 0,026)
	6	0,793 (± 0,032)
150	**1**	0,086 (± 0,001)
	3	0,320 (± 0,003)
	6	0,528 (± 0,020)

Comparing the results from both measurements and the analysis of the difference between them can be observed in Table 5, where this phenomenon is witnessed.

Table 5 Comparison of the displacement from the information of the Laser and that of the image processing.

Frequency (Hz)	Amplitude (V)	Laser displacement (mm)	Video displacement (mm)	Difference	Difference (%)
25	1	0,150 (± 0,004)	0,243 (± 0,09)	0,093	61,99%
	3	0,552 (± 0,006)	0,445 (± 0,09)	0,107	19,42%
	6	1,225 (± 0,034)	0,879 (± 0,09)	0,346	28,27%
50	1	0,159 (± 0,003)	0,232 (± 0,09)	0,073	46,13%
	3	0,562 (± 0,019)	0,650 (± 0,09)	0,088	15,65%
	6	1,082 (± 0,011)	0,991 (± 0,09)	0,091	8,43%
75	1	0,173 (± 0,003)	0,216 (± 0,09)	0,043	24,89%
	3	0,744 (± 0,009)	0,771 (± 0,09)	0,027	3,62%
	6	1,257 (± 0,018)	1,219 (± 0,09)	0,038	3,04%
100	1	0,210 (± 0,004)	0,232 (± 0,09)	0,022	10,27%
	3	0,774 (± 0,007)	0,782 (± 0,09)	0,008	1,04%
	6	1,281 (± 0,041)	1,181 (± 0,09)	0,100	7,82%
125	1	0,146 (± 0,002)	0,223 (± 0,09)	0,077	52,96%
	3	0,504 (± 0,026)	0,444 (± 0,09)	0,060	11,85%
	6	0,793 (± 0,032)	0,671 (± 0,09)	0,122	15,34%
150	1	0,086 (± 0,001)	0,108 (± 0,09)	0,022	25,85%
	3	0,320 (± 0,003)	0,344 (± 0,09)	0,024	7,62%
	6	0,528 (± 0,020)	0,447 (± 0,09)	0,081	15,32%

From this comparison, the reliability of the procedure used for the LDV data acquisition is checked, in order to study the test cell displacement properly. This means that it is possible to trust the procedure used to obtain the data from the LDV. Nevertheless, the system will always have some error in the measurements, computed as *noise*, which, in this case, corresponds to an average of around 15% of the LDV measurement.

3.2. High frequencies: study of the Test Cell

As showed in Table 2, the test cell is subjected to different conditions. Further, a frequency study of two different cells of the grid is also performed. This study,

followed by the results obtained from the displacement and the attenuation, are detailed in the following subsections.

3.2.1. Displacement

Applying the experimental procedure and analysis explained in sections 2.3 and 2.4 respectively, the first observations made in the displacement study is that the test cell is affected at every point analysed, i.e. each cell of the grid.

The first observation from the displacement of the walls computed is that it tends to increase as far as the amplitude of the waveform generator is increased. This means that at 6V; the maximum voltage that can be applied by the waveform generator with the amplifier connected to it (see section 2.2), the displacement is 10 times bigger than the displacement of the walls at 1V. The noise computed in all the cases is around 0,002 μm.

Within these terms, if the displacement is compared with the amplitude observed, it is observed that the displacement is more lineal on the face of the piezoelectric than on the back, and the displacements obtained on the face side are almost twice of those obtained on the back. These phenomena are shown in Figures 3.1-3.6, where the evolution of the displacement as far as the amplitude in increased, for six different conditions: face-empty, face-half, face-full, back-empty, back-half and back-full, is shown.

The face and the back refer to the wall which holds the piezoelectric (face) and also the other side (back). The other conditions refer to how much distilled water the test cell contains: without water (empty), full of water, half full of water. For more details about the conditions see section 2.3.2 and Table 2.

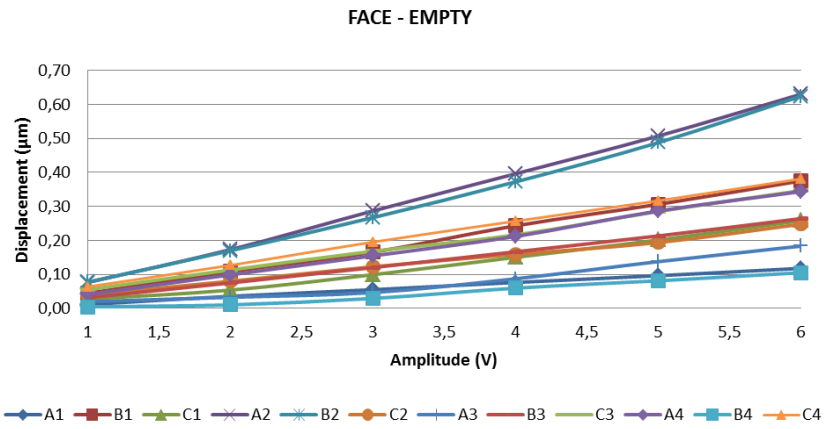

Figure 3.1 Displacement (μm) as a function of the amplitude (V) applied at 53kHz for the face of the test cell while empty.

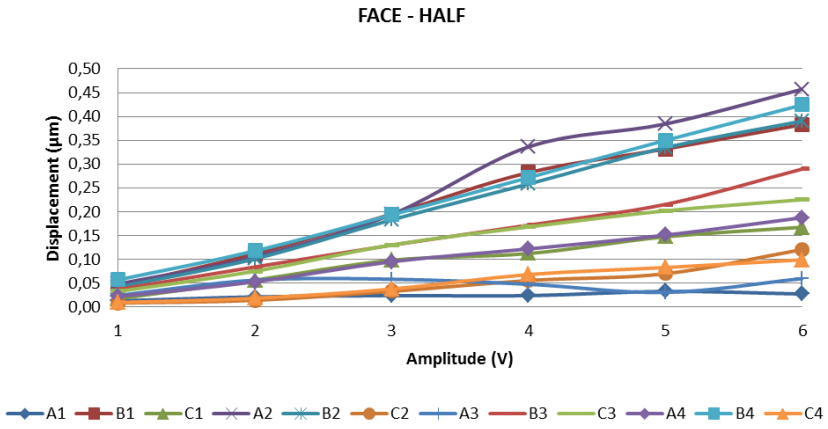

Figure 3.2 Displacement (µm) as a function of the amplitude (V) applied at 53kHz for the face of the test cell while half full of water.

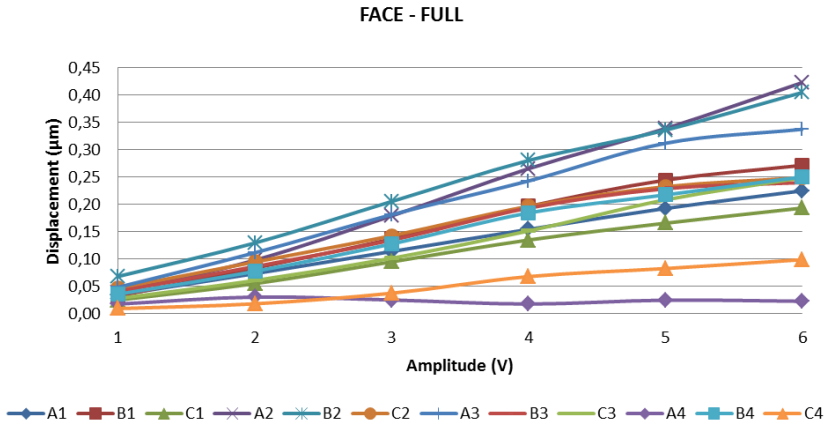

Figure 3.3 Displacement (µm) as a function of the amplitude (V) applied at 53kHz for the face of the test cell while full of water.

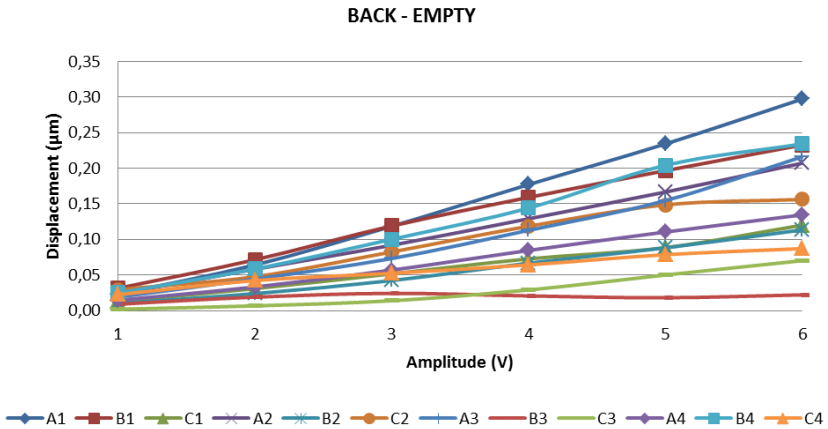

Figure 3.4 Displacement (µm) as a function of the amplitude (V) applied at 53kHz for the back of the test cell while empty.

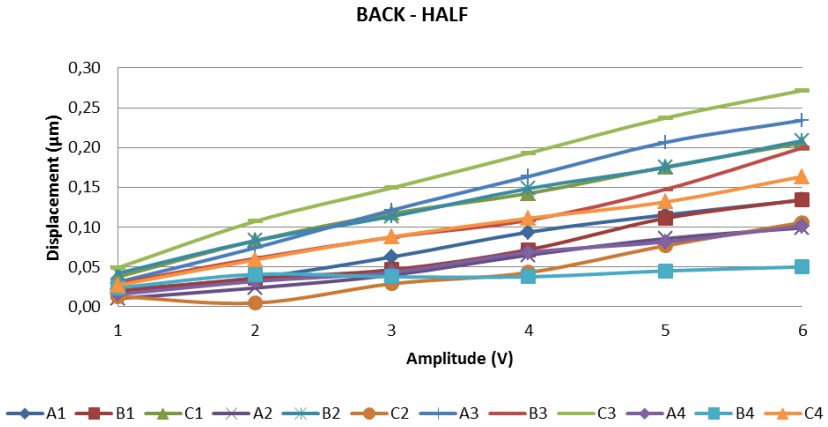

Figure 3.5 Displacement (µm) as a function of the amplitude (V) applied at 53kHz for the back of the test cell while half full of water.

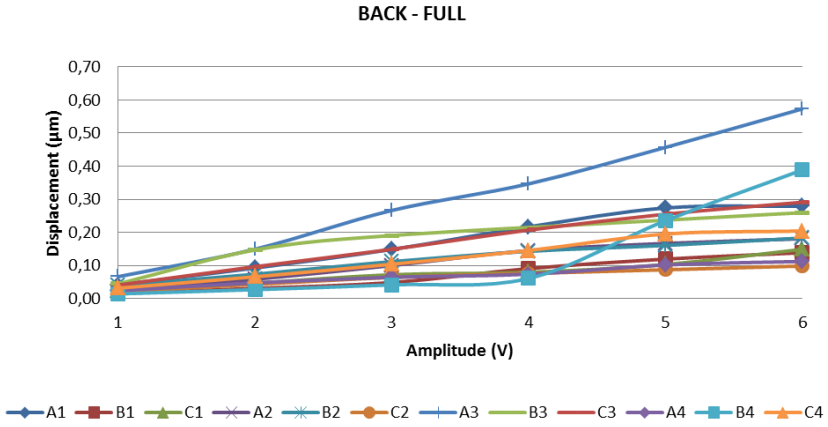

Figure 3.6 Displacement (µm) as a function of the amplitude (V) applied at 53kHz for the back of the test cell while full of water.

Therefore, comparing the displacement of every cell at the different amplitudes and conditions, a different behaviour is observed. In this case, more displacement in the corners of the test cell (A1, A3, C1 and C3) is received. Also, generally, there is more displacement in the face part, especially when it is empty. There is more displacement in the back part only when it is full, and only in one corner of the test cell. This is due to the fluid within it, which transports the acoustic field. In the rest of the cases, the bigger displacement corresponds to the face-empty condition.

This behaviour is observed in Figures 3.7-3.12, where the displacement of each cell for the different conditions (face-empty, face-half, face-full, back-empty, back-half and back-full) for the different amplitudes, all at 53 kHz is shown. In order to understand the legend of the Figures 3.7-3.12, Table 6 details the number given to each cell.

Table 6 Numbers given to each cell of the grid of the test cell applied in Figures 3.7-3.12.

CELLS	***A1***	*1*	***A2***	*4*	***A3***	*7*	***A4***	*10*
	B1	2	**B2**	5	**B3**	8	**B4**	11
	C1	3	**C2**	6	**C3**	9	**C4**	12

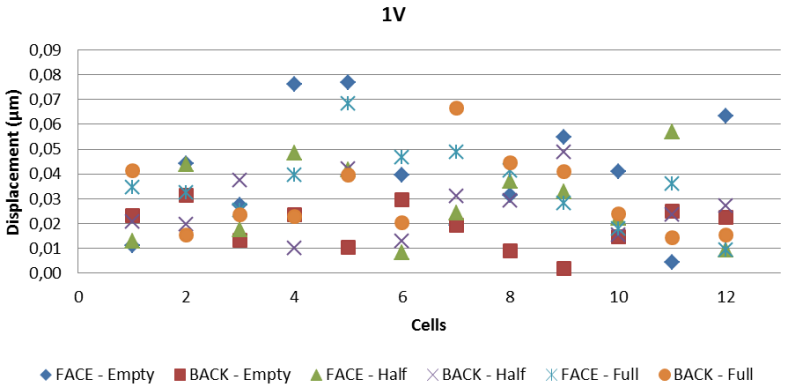

Figure 3.7 Displacement (µm) of each cell (see Table 6) of the test cell at different conditions at 1V.

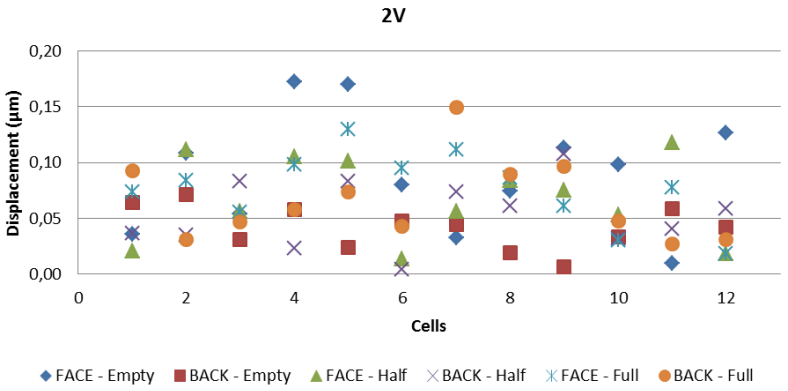

Figure 3.8 Displacement (µm) of each cell (see Table 6) of the test cell at different conditions at 2V.

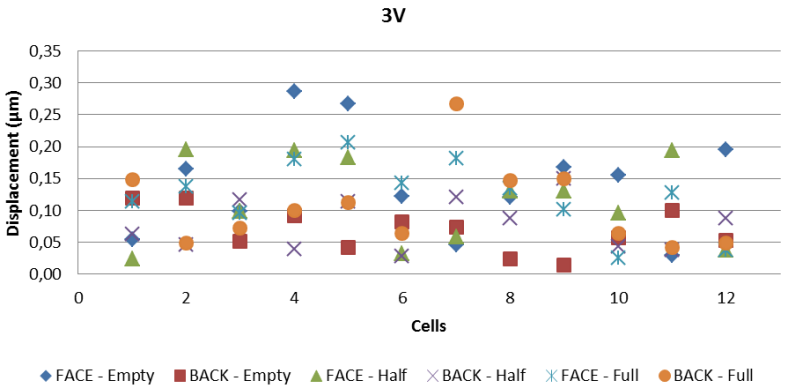

Figure 3.9 Displacement (µm) of each cell (see Table 6) of the test cell at different conditions at 3V.

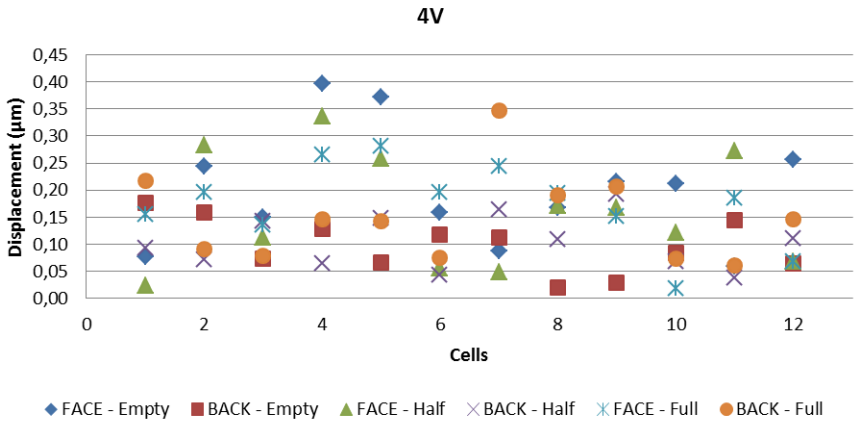

Figure 3.10 Displacement (µm) of each cell (see Table 6) of the test cell at different conditions at 4V.

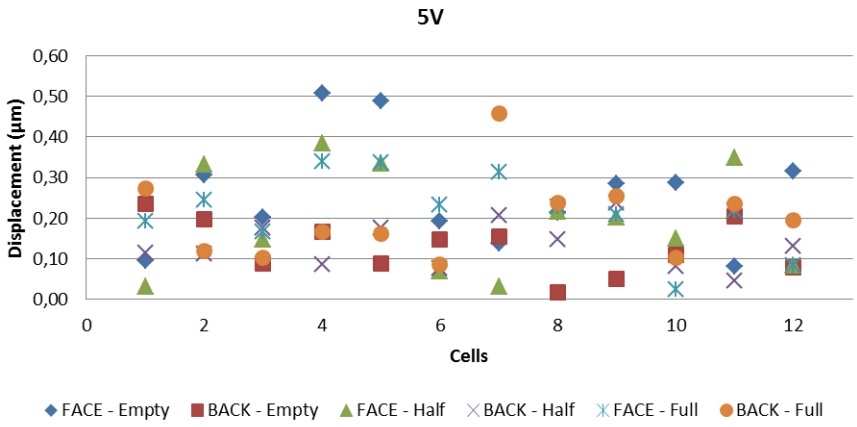

Figure 3.11 Displacement (µm) of each cell (see Table 6) of the test cell at different conditions at 5V.

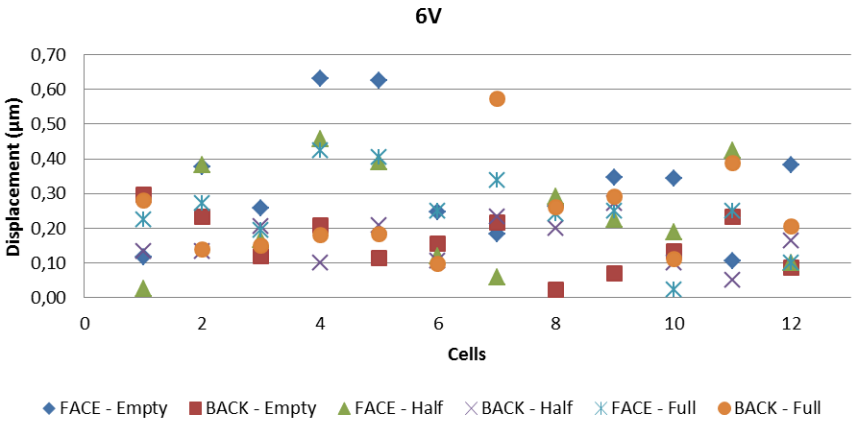

Figure 3.12 Displacement (µm) of each cell (see Table 6) of the test cell at different conditions at 6V.

From Figures 3.7-3.12, it can be observed that the cells that have more displacement are those with the conditions of *face empty*, especially for A2 and B2, which are very close to the source of the vibration (piezoelectric). Nevertheless, in general, the face-empty condition has the most displacement in almost all the cells, with only two exceptions; in the case of *back-full*, which can be observed in a corner of the test cell and in *face-half* condition, which is in B1 and B4, the middle part of the test cell.

Apart from these figures, to be able to observe the distribution of the displacement along the wall is very important at any condition. For this purpose, a displacement map of the wall for all the conditions has been generated from the measurements of each cell. These displacement maps show the distribution of the displacement along the wall of the test cell, for the different cells giving a 2D image of the different displacements with a scale of colours. The displacement maps for 6V of the distribution along the walls of the test cell are displayed in Figures 3.13-3.15, taking into account that the data displayed corresponds to the centre point of each cell but is only represented by the corner points. The displacement maps at different amplitudes are presented in the Annex of this document.

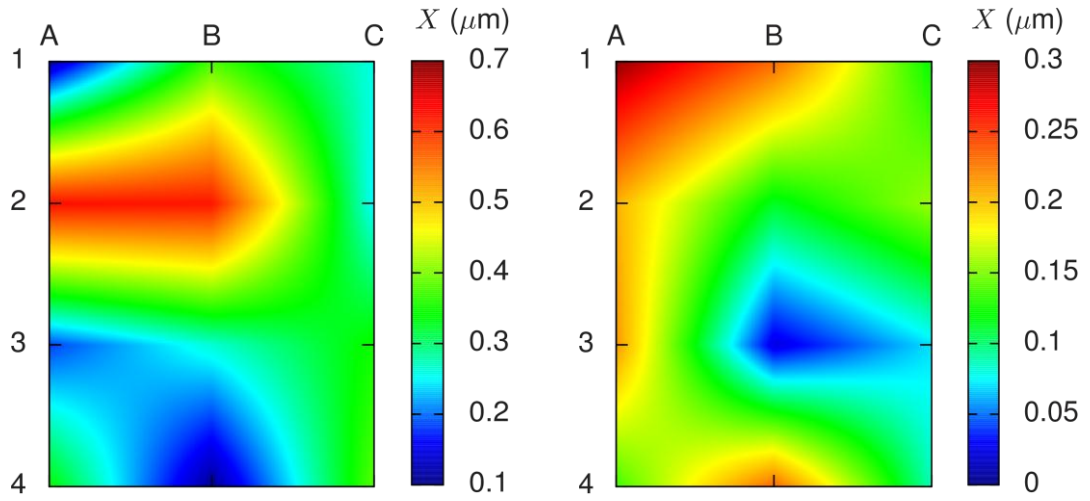

Figure 3.13 Displacement maps in µm of the face and back walls of the test cell empty of water at 6V.

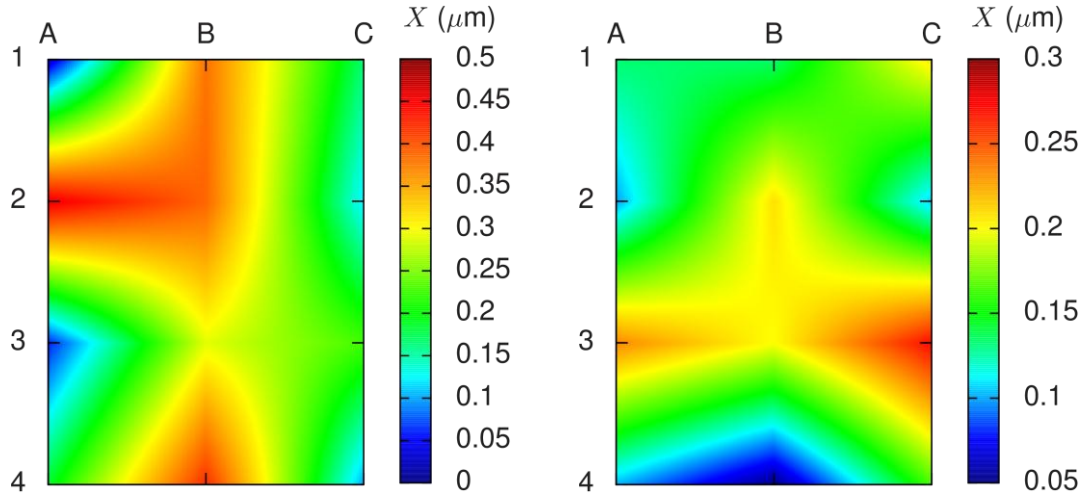

Figure 3.14 Displacement maps in µm of the face and back walls of the test cell half full of water at 6V.

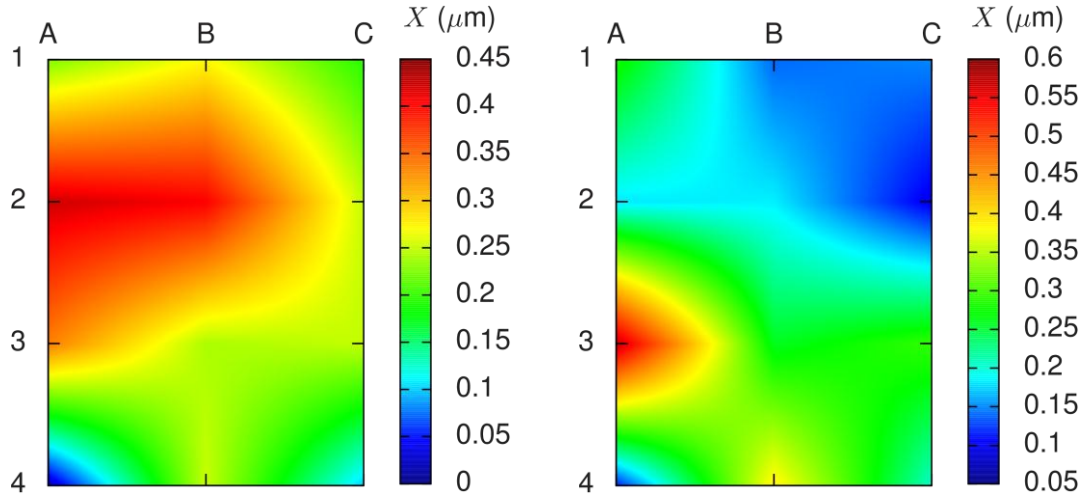

Figure 3.15 Displacement maps in µm of the face and back walls of the test cell full of water at 6V.

From the displacement maps, showed in Figures 3.13-3.15, the following behaviours are generally observed. On one side, the face side, vibrational displacement is seen highly concentric to the top of the source of the vibrations, which corresponds to the cell B2. This behaviour is especially observed when the test cell is empty.

On the other side, some displacement with the increase in water is observed on the back side. Therefore, higher amounts of water forces displacement to occur concentrically to one side, very close to the source of the vibration, which in this case corresponds to the cell A3.

Comparing both sides, different patterns are observed from the displacement maps. However, it must be taken into account that when comparing both sides, the exact opposite must not be compared. Instead, what must be compared are the opposing corner ends. For example; face side A1 with back side C1, face side B1 with back side B1 and face side C1 with back side A1. The direct comparison of that will be observed in the following section 3.2.2.

Besides, from the displacement maps at different amplitudes presented in the Annexes, it is observed that the behaviour of the walls is generally similar in all the amplitudes, with the only difference being an increase in magnitude of displacement when the amplitude is increased. This is particularly observed at 1V. In this case, the displacement observed is largely smaller than in the case of 6V, and, due to the fact that all the cases use the same legend, almost no displacement is observed on the back wall. In this last case, a small displacement is observed when the test cell is full of water, due to it being affected with a heavier fluid medium inside.

3.2.2. Attenuation

The attenuation is a gradual loss in intensity through a medium and it affects the propagation of waves. In this case, the acoustic attenuation is calculated in order to know the difference between the acoustic wave which affects the face wall, where the vibrating source is situated, and the opposite.

The acoustic attenuation can be expressed as the division between the pressure 'P' at a given point by the pressure at the beginning, which is proportional to the distance 'Δx' and the attenuation coefficient 'α'.

$$\frac{P(x+\Delta x)}{P(x)} = e^{-\alpha \Delta x} \tag{3.1}$$

As mentioned in section 1.1.1, the amplitude of the acoustic pressure is related with the amplitude of the acoustic displacement of the acoustic wave. This relationship is also introduced in Equation 1.3. Therefore, interpreting Equation 3.1 describes that, if the differences between the displacement of the back wall and the

face wall for all is constant, the test cell has an expected attenuation, generated by the medium containing the test cell.

Following the method of comparison of both corner ends, as described before, is shown in Tables 7-9, where the difference between the corresponding cells, computing the division between them, and using Equation 3.1 for the calculation of the attenuation factor α for the different conditions of the medium within the test cell, and the different amplitudes at 53 kHz is detailed. The cells have been ordered in a numerical order.

Table 7 Attenuation coefficient for empty test cell.

Empty											
1V		2V		3V		4V		5V		6V	
Cell	α	Cell	α	Cell	α	Cell	α	Cell	α	Cell	α
C3b/A3f	2,52E-05	B2b/B2f	2,17E-05	B2b/B2f	2,05E-05	B3b/B3f	2,32E-05	B3b/B3f	2,74E-05	B3b/B3f	2,75E-05
B2b/B2f	2,23E-05	C3b/A3f	1,75E-05	B3b/B3f	1,77E-05	B2b/B2f	1,91E-05	B2b/B2f	1,90E-05	B2b/B2f	1,89E-05
A4b/C4f	1,62E-05	B3b/B3f	1,52E-05	C2b/A2f	1,38E-05	C2b/A2f	1,34E-05	C4b/A4f	1,44E-05	C2b/A2f	1,55E-05
B3b/B3f	1,38E-05	A4b/C4f	1,48E-05	A4b/C4f	1,37E-05	C4b/A4f	1,32E-05	C2b/A2f	1,36E-05	C4b/A4f	1,53E-05
A3b/C3f	1,17E-05	C2b/A2f	1,43E-05	C3b/A3f	1,34E-05	A4b/C4f	1,23E-05	A4b/C4f	1,17E-05	A4b/C4f	1,16E-05
C2b/A2f	1,05E-05	A3b/C3f	1,04E-05	C4b/A4f	1,20E-05	C3b/A3f	1,22E-05	C3b/A3f	1,12E-05	C3b/A3f	1,06E-05
C4b/A4f	6,61E-06	C4b/A4f	9,38E-06	A3b/C3f	9,23E-06	A3b/C3f	7,22E-06	A3b/C3f	6,80E-06	B1b/B1f	5,31E-06
A2b/C2f	5,80E-06	B1b/B1f	4,60E-06	B1b/B1f	3,64E-06	B1b/B1f	4,71E-06	B1b/B1f	4,92E-06	A3b/C3f	5,25E-06
B1b/B1f	3,74E-06	A2b/C2f	3,51E-06	A2b/C2f	3,20E-06	A2b/C2f	2,32E-06	A2b/C2f	1,67E-06	A2b/C2f	1,99E-06
A1b/C1f	1,86E-06	C1b/A1f	1,51E-06	C1b/A1f	6,57E-07	C1b/A1f	5,15E-07	C1b/A1f	9,04E-07	C1b/A1f	-2,24E-07
C1b/A1f	-1,74E-06	A1b/C1f	-2,00E-06	A1b/C1f	-2,00E-06	A1b/C1f	-1,83E-06	A1b/C1f	-1,69E-06	A1b/C1f	-1,56E-06
B4b/B4f	-1,93E-05	B4b/B4f	-1,96E-05	B4b/B4f	-1,37E-05	B4b/B4f	-9,84E-06	B4b/B4f	-1,03E-05	B4b/B4f	-8,90E-06

Table 8 Attenuation coefficient for half full test cell.

Half											
1V		2V		3V		4V		5V		6V	
Cell	α	Cell	α	Cell	α	Cell	α	Cell	α	Cell	α
C2b/A2f	1,48E-05	C2b/A2f	3,49E-05	C2b/A2f	2,12E-05	C2b/A2f	2,29E-05	B4b/B4f	2,28E-05	B4b/B4f	2,38E-05
B4b/B4f	9,75E-06	B1b/B1f	1,28E-05	B4b/B4f	1,82E-05	B4b/B4f	2,20E-05	C2b/A2f	1,79E-05	C2b/A2f	1,63E-05
B1b/B1f	8,99E-06	B4b/B4f	1,18E-05	B1b/B1f	1,60E-05	B1b/B1f	1,52E-05	B1b/B1f	1,22E-05	B1b/B1f	1,16E-05
B3b/B3f	2,58E-06	A1b/C1f	4,91E-06	B2b/B2f	5,32E-06	B2b/B2f	6,15E-06	B2b/B2f	7,21E-06	B2b/B2f	6,96E-06
A3b/C3f	6,29E-07	B3b/B3f	3,63E-06	A1b/C1f	5,03E-06	B3b/B3f	5,09E-06	B3b/B3f	4,21E-06	B3b/B3f	4,14E-06
B2b/B2f	-7,96E-08	B2b/B2f	2,22E-06	B3b/B3f	4,40E-06	A1b/C1f	2,01E-06	A1b/C1f	2,73E-06	A1b/C1f	2,48E-06
A1b/C1f	-1,97E-06	A3b/C3f	1,79E-07	C4b/A4f	9,13E-07	C4b/A4f	1,03E-06	C4b/A4f	1,53E-06	A2b/C2f	2,19E-06

C4b/A4f	-2,25E-06	C4b/A4f	-1,20E-06	A3b/C3f	7,96E-07	A3b/C3f	3,02E-07	A4b/C4f	2,03E-07	C4b/A4f	1,53E-06
A2b/C2f	-2,45E-06	A2b/C2f	-5,66E-06	A4b/C4f	-1,53E-06	A4b/C4f	0,00E+00	A3b/C3f	-2,45E-07	A4b/C4f	-2,66E-07
A4b/C4f	-5,43E-06	A4b/C4f	-6,14E-06	A2b/C2f	-2,08E-06	A2b/C2f	-1,72E-06	A2b/C2f	-2,24E-06	A3b/C3f	-4,36E-07
C3b/A3f	-7,77E-06	C3b/A3f	-7,13E-06	C3b/A3f	-1,05E-05	C3b/A3f	-1,55E-05	C1b/A1f	-1,87E-05	C3b/A3f	-1,69E-05
C1b/A1f	-1,20E-05	C1b/A1f	-1,52E-05	C1b/A1f	-1,77E-05	C1b/A1f	-1,99E-05	C3b/A3f	-2,27E-05	C1b/A1f	-2,25E-05

Table 9 Attenuation coefficient for full test cell.

Full											
1V		**2V**		**3V**		**4V**		**5V**		**6V**	
Cell	**α**	**Cell**	**α**	**Cell**	**α**	**Cell**	**α**	**Cell**	**α**	**Cell**	**α**
B4b/B4f	1,03E-05	B4b/B4f	1,17E-05	B4b/B4f	1,25E-05	C2b/A2f	1,39E-05	C2b/A2f	1,51E-05	C2b/A2f	1,62E-05
B1b/B1f	8,39E-06	B1b/B1f	1,11E-05	B1b/B1f	1,15E-05	B4b/B4f	1,23E-05	B2b/B2f	8,21E-06	B2b/B2f	8,83E-06
A2b/C2f	7,95E-06	C2b/A2f	9,19E-06	C2b/A2f	1,15E-05	C3b/A3f	2,70E-06	B1b/B1f	7,96E-06	B1b/B1f	7,47E-06
C2b/A2f	7,29E-06	B2b/B2f	6,28E-06	B2b/B2f	6,77E-06	B3b/B3f	1,74E-07	C1b/A1f	6,96E-06	C1b/A1f	4,59E-06
B2b/B2f	6,07E-06	A2b/C2f	5,42E-06	C1b/A1f	5,06E-06	B1b/B1f	8,58E-06	A2b/C2f	3,71E-06	A2b/C2f	3,56E-06
C1b/A1f	4,22E-06	C1b/A1f	5,02E-06	A2b/C2f	3,97E-06	B2b/B2f	7,50E-06	C3b/A3f	3,05E-06	C3b/A3f	2,92E-06
C3b/A3f	1,00E-06	C3b/A3f	2,50E-06	C3b/A3f	2,34E-06	C1b/A1f	7,42E-06	B3b/B3f	-3,94E-07	B3b/B3f	-8,68E-07
B3b/B3f	-8,58E-07	A1b/C1f	-5,72E-06	B3b/B3f	-9,71E-07	A2b/C2f	3,36E-06	B4b/B4f	-8,83E-07	A4b/C4f	-1,39E-06
A1b/C1f	-5,52E-06	B3b/B3f	-3,42E-07	A1b/C1f	-4,95E-06	A4b/C4f	-8,48E-07	A4b/C4f	-2,28E-06	A1b/C1f	-4,07E-06
C4b/A4f	-6,31E-06	C4b/A4f	-8,54E-06	A4b/C4f	-5,96E-06	A1b/C1f	-5,26E-06	A1b/C1f	-5,57E-06	B4b/B4f	-4,88E-06
A3b/C3f	-9,50E-06	A3b/C3f	-9,96E-06	A3b/C3f	-1,07E-05	A3b/C3f	-9,19E-06	A3b/C3f	-8,71E-06	A3b/C3f	-9,26E-06
A4b/C4f	-1,03E-05	A4b/C4f	-1,06E-05	C4b/A4f	-1,57E-05	C4b/A4f	-2,33E-05	C4b/A4f	-2,29E-05	C4b/A4f	-2,43E-05

From Tables 7-9, the following can be observed. First of all, the attenuation is bigger when the test cell is full of water. That is due to the density of the fluid phase between the walls of the test cell. The amount of mass of water situated between the walls generates acoustic waves that would need to propagate with more effort in order to reach the other wall with maximum effectiveness.

Secondly, in the ‘empty’ case, the smaller attenuation factor is in cell B2 and B3, where the vibrating source is located. These cells compute the maximum displacement on the face walls, as can be seen in the displacement maps of section 3.2.1. In the cases of half and full of water, the area with the minimum difference is on one side (back C2/face A2) and B4, which are related with the maximum face displacement in those conditions, especially in the case of C2/A2.

Bigger attenuation factors in the case of an empty test cell are observed in the cell B4, just under the vibrating source, while in the cases of half and full, the maximum differences correspond to the corners of the test cell, especially C1/A1, for the half case, and C4/A4 for the case of full case.

As can be seen, in general, the difference between both displacements, the face wall and back wall, is not constant along the test cell, and hence the test cell has an unpredicted attenuation, which does not correspond to the maximum displacement obtained in the wall observed from the displacement maps.

The attenuation coefficient for water is 0,0022 dB/(MHz·cm) [16]. The attenuation coefficient computed at Tables 7-9 has been calculated from the values of displacement in μm. For that reason, converting to μm, the attenuation coefficient for water is 2,2 x 10^{-7} dB/(MHz·μm). The attenuation coefficient for the air at 20ºC is 1,64 x 10^{-4} dB/(MHz·μm) [17]. Comparing these values with the obtained attenuation coefficients from Table 7-9, confirms the absence of a specific attenuation phenomenon.

3.2.3. Frequency

Despite all the measurements carried out before being performed at 53 kHz, a frequency study of two points of the test cell has also been performed. The main purpose of this frequency study is to observe the evolution of the displacement of the test cell as the frequency changes.

In order to do that, two points of the test cell have been chosen, and the evolution as a function of the frequency applied to the vibrating source has been measured. The ranges of frequencies measured are detailed in Table 10. The points chosen are: a corner of the test cell (C1/A1) and the location of the vibrating source (B3). The point C1/A1 follows the method of comparison of both corner ends, introduced before. Figure 3.16 shows where the analysis of the frequency took place. The part in purple corresponds to cell B3. The part in orange corresponds to C1/A1.

Table 10 Range of frequencies in kHz measured.

Frequencies (kHz)																			
5	6	7	8	9	10	15	20	25	30	35	40	45	47	49	50	51	52	53	54
55	57	60	65	70	75	80	85	90	95	110	120	130	135	140	150	160	170	190	200
High frequencies (kHz) :						660	680	700	730	750									

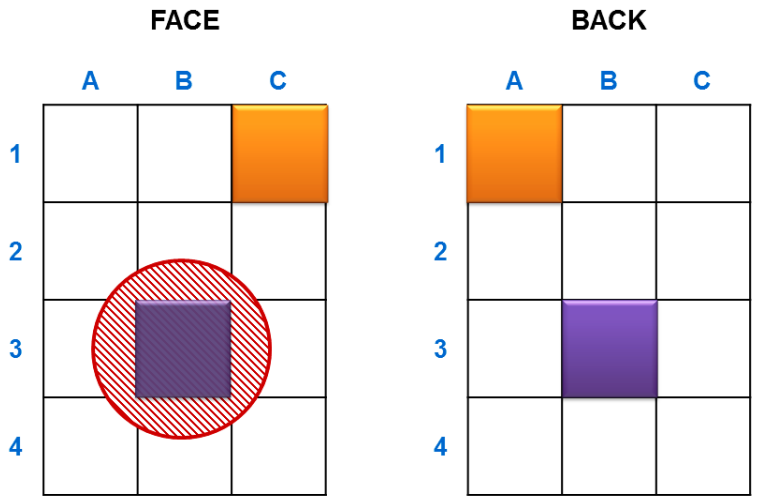

Figure 3.16 Positioning scheme of the frequency study of the test cell. Purple is for the cell B3 in the centre of the piezoelectric, and in orange, the cell C1/A1 in a corners of the test cell.

Figures 3.17-3.22 show the evolution of the displacement, in μm, as a function of the frequency applied for the cell B3, indicated in purple in Figure 3.31, on both sides with different media. The frequency is from 5kHz to 200kHz and it is expressed in a logarithmic scale.

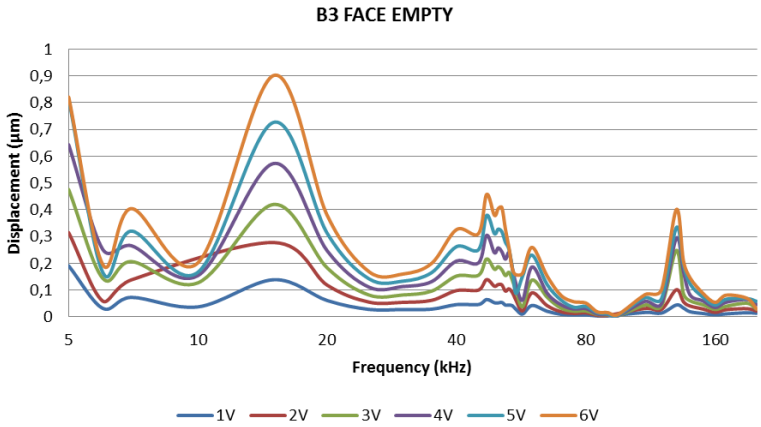

Figure 3.17 Displacement in μm as a function of the frequency in kHz applied in logarithmic scale for B3 cell in face empty conditions.

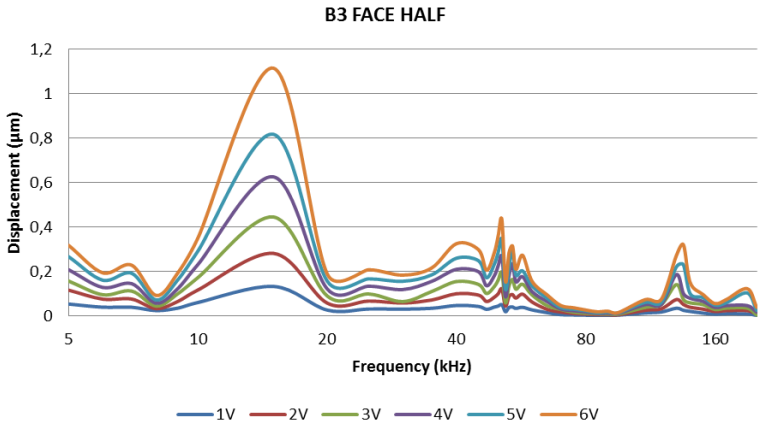

Figure 3.18 Displacement in µm as a function of the frequency in kHz applied in logarithmic scale for B3 cell in face half full of water conditions.

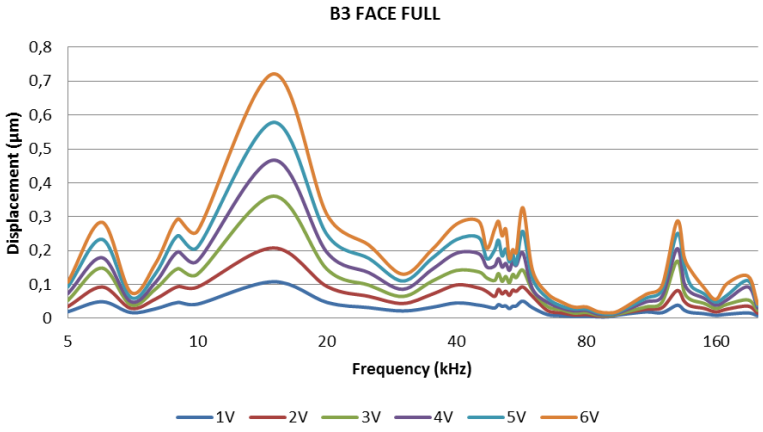

Figure 3.19 Displacement in µm as a function of the frequency in kHz applied in logarithmic scale for B3 cell in face full of water conditions.

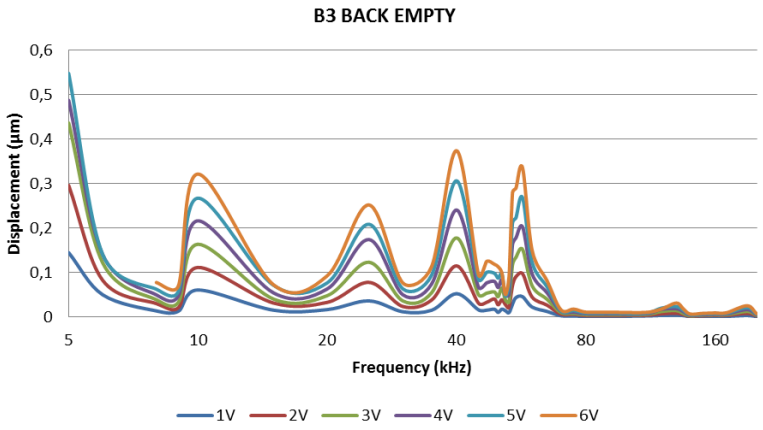

Figure 3.20 Displacement in µm as a function of the frequency in kHz applied in logarithmic scale for B3 cell in back empty conditions.

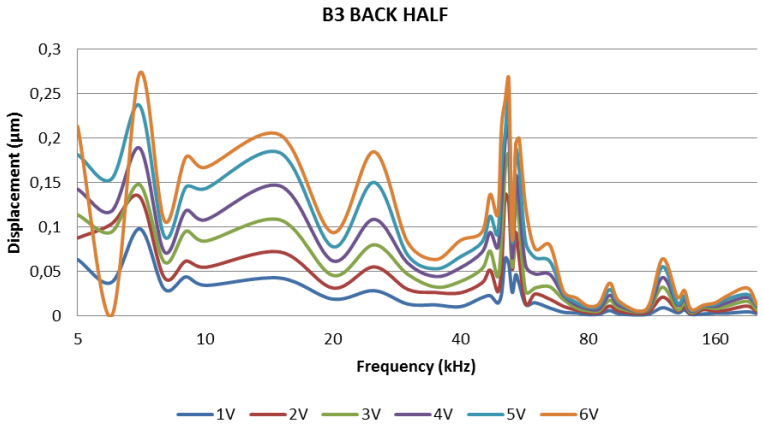

Figure 3.21 Displacement in µm as a function of the frequency in kHz applied in logarithmic scale for B3 cell in back half full of water conditions.

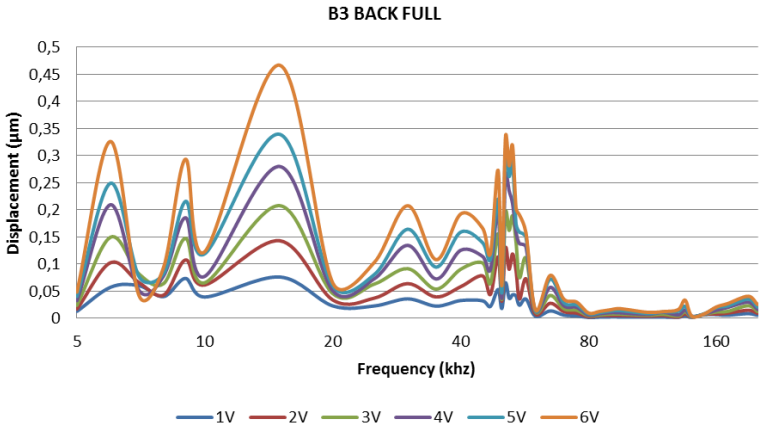

Figure 3.22 Displacement in µm as a function of the frequency in kHz applied in logarithmic scale for B3 cell in back full of water conditions.

Observing the evolution of the displacement as the frequency changes at B3 from Figures 3.17-3.22, where the vibration source is located, some patterns are observed. The first observation is related with the low frequencies, from 5 kHz to 20 kHz, in which the vibrating source, in this case the piezoelectric, is audible to human ears. At this region, the maximum displacements are observed.

After this, the region where the vibration source is no longer audible starts and some displacement can be observed. The displacements observed here are between 0,05 µm to 0,43 µm for both sides at half and empty conditions. However, at full conditions, the displacements observed are between 0,015 µm to 0,32 µm. This is due to the heavier fluid medium contained in the test cell; Water. The Figure 3.23 shows the evolution of the frequency, specifically at 30-60 kHz region, for B3 cell, for the conditions of *face-empty*. The Figures corresponding to all the other conditions measured are located in the Annexes of this document.

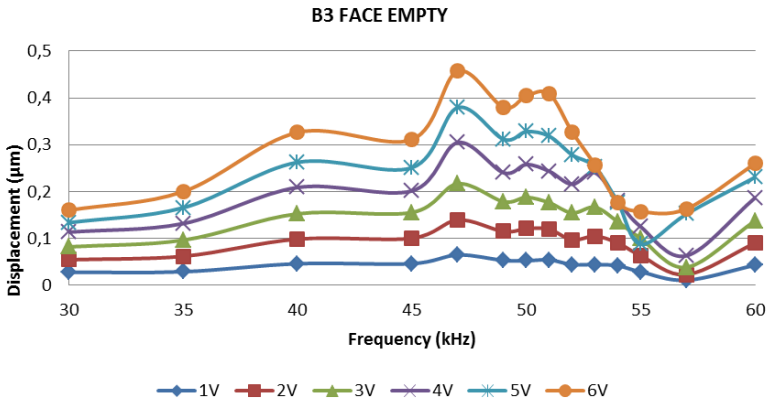

Figure 3.23 Displacement in µm as a function of the frequency at 30-60 kHz region for B3 cell at face empty conditions.

From Figure 3.23, inside the evolution of the frequency within this region of 30-60 kHz, it is observed that the maximum displacement is not situated at the radial resonance frequency of the piezoelectric, which corresponds to 53 kHz.

This behaviour ends around 85 kHz, wherein all cases, a minimum displacement of the walls are measured. After that point, there is an increase in the displacement around 130 kHz. This increase of displacement becomes more notable at the face side, which has a peak of 0,28 µm in full and half, and 0,4 µm in empty condition, than at the back side, which has a maximum of 0,16 µm. However, in the case of half filled, the displacement is very similar on both sides. The only difference is that at the back side, the maximum peak of that region advanced to 120 kHz, while on the face side, it is still at 130-135 kHz.

Computing the frequency at which the acoustic wave propagates along the test cell, the following formula is applied:

$$f = \frac{v}{\lambda} \tag{3.2}$$

Where the frequency 'f' is the result of the division between the velocity of the acoustic wave, 'v', and the wavelength 'λ'. Being that the wavelength is proportional to the length of the test cell, which in this case is 9 cm (see section 2.1.2), the frequency of the test cell at the conditions of empty and full of water has been calculated.

In the case of empty of water, which contains air, and assuming a wave velocity of 340 m/s, the frequency obtained is around 3,8 kHz. In that condition, in Figure 3.17, a tendency to have a peak of displacement around 3 kHz can be observed. On the other hand, in full of water conditions, and assuming a wave velocity of 1400 m/s, the frequency obtained is around 15,5 kHz. From Figure 3.19 the same behaviour is observed; the maximum displacement is found to be around 15 kHz. In the case of half full of water, the behaviour of the maximum displacement is not able to be compared with the frequency due to the conditions of having two

phase flows in the same container. This phenomenon shows that the resonant frequency of the test cell and the medium container is more relevant than the resonant frequency of the piezoelectric, to study the displacement evolution as a function of the frequency.

Regarding the corner side of the test cell (C1/A1), where, in Figure 3.16, it is highlighted with orange, the same measurements have been taken. Nevertheless, from the measurements of the evolution of the displacement as a function of the frequency and the amplitude applied, the figures can be found in the Annexes of this document. Also, the evolution of the frequency, specifically at the 30-60 kHz region, for this case, in a corner side of the test cell is included in the Annex.

From the figures referring to the evolution of the displacement at the corner of the test cell, some differences are observed, compared with the ones from the cell B3. At the corner, for low frequencies, from 5 kHz to 20 kHz a big displacement does not exist, and the maximum displacement happens between 30-60 kHz for all the cases. In the figures which show that region, where the radial frequency of the piezoelectric is placed, it can be observed that the maximum displacement is very similar, and is 0,21 μm, despite the case of the face empty condition in C1, where this value is bigger.

Also, in the evolution of the frequency, at around 125-130 kHz, the displacement of the wall increases in all conditions, the case of empty being the one that achieve more displacement, followed by the half and the full conditions.

The high frequency study, which correspond to the surroundings of the lateral resonance frequency of the piezoelectric, 680-730 kHz, has been measured but not computable due to the noise added to the system for environmental reasons.

Chapter 4

CONCLUSIONS AND FUTURE LINES

After the experimentation and observations, it is clear that acoustic fields do indeed have an effect on the outer surfaces of the object under the influence of an acoustic field. Therefore, when attempting to control bubbles in aerospace applications, both without and under the influence of microgravity, it was important to have performed these tests in order to check the behaviour of the surface of an object under the effects of an acoustic field. This section will entail the summary of all the observations made in these series of experiments.

The goal of this project was to experimentally study the various effects that acoustic fields of varying magnitudes have on a defined test cell containing fluid media of different volumes, using very high precision *Laser Doppler Vibrometry*, in order to use this data in future scientific research involving acoustic behaviour on a rigid body containing fluids. In order to accomplish this goal, an experiment has been designed, built, carried out and analysed using an LDV, a vibration-free structure, a test shaker, a test cell, a source of vibration (piezoelectric) and the output instruments.

From the study of the shaker, the reliability of the procedure of acquisition of the data from the LDV was checked. This meant that it was possible to trust the procedure used in order to obtain the data from the LDV even if there was some error in the measurements, the *noise*, which was around 15% of the measurement.

From the study of the test cell, observations were found and divided into three sections; displacement, attenuation and frequency.

Regarding the displacement, the first observation was an increase in magnitude of displacement of the walls when there was an increase in the applied amplitude. Here, the noise computed in all the cases was found to be around 0,002 μm. Furthermore, the displacement was more linear on the face of the piezoelectric than on the back, and the displacements obtained on the face side were almost twice of those obtained on the back. More displacement in the corners of the test cell was received. Also, generally, there was more displacement in the face part, especially when it was empty due to the fluid within it.

An analysis of the displacement maps were carried out to get clearer image of the displacement at the different cells of the walls for the different conditions analysed. On the face side, vibrational displacement was seen highly concentric to the top of the source of the vibrations, especially when the test cell was empty. However, the back side showed some displacement with the increase in water and higher amounts of water forced displacement to occur concentrically to one side, close to the source of the vibration.

The next experimentation done was a calculation of the attenuation, in order to see if the wave transmitted was received effectively by the other wall, when passing through the medium between them, and to compute the coefficient of this loss. The observations were that the attenuation was bigger when the test cell was full of water because of the density of the fluid phase between the walls. Although, when the test cell was empty, the minimum difference between the back and the face was seen located at the point of the vibrating source. The attenuation coefficient was not constant along the test cell, and hence the test cell had an unpredicted attenuation, which did not correspond to the maximum displacement obtained in the wall.

Regarding the frequency study and how it affected displacement in two points of the test cell, the centre and a corner, four distinct observations were made. Firstly, when measuring the displacement at the centre of the test cell, there was a range of frequencies that caused a large displacement, and during this range, a loud audible sound was produced by the piezoelectric. This maximum displacement at this region of frequencies did not appear when the measurement was taken at the corner of the test cell. The second observation showed that many peaks of displacement were generated around the region of radial resonance, although, this displacement was not maximum at the theoretical value of 53 kHz. The third observation showed slight displacements around the same region, 120-130 kHz, for both measurements; the centre and the corner. Finally, the fourth observation shows that the resonant frequency of the test cell and the medium container is more relevant than the resonant frequency of the piezoelectric, due to maximum displacements around the resonant frequency of the test cell calculated for different media is observed.

As can be seen from the observations above, the object subjected to vibrations was clearly affected, even in the slightest, by the acoustic field. This could be characterized by the fluid media within the object, the shape of the object, the material characteristics of the object and the characteristics of the acoustic field itself. These points could serve as parameters to be taken into account for future experiments to control bubbles with an acoustic field in aerospace research. That means experiments carried out with a test cell of different shape and size, different fluids within in it, like oils, spirits and maybe coagulants.

Furthermore, these experiments could be expanded to a large scale investigation in microgravity using prototype propellant storage containers, for real life implementation in aerospace exploration and future space missions.

REFERENCES

[1] R. Mattsson, “Bending and acoustic waves in a water filled box studied by pulsed TV holography and LDV”, *Optics and Lasers in Engineering, 44*, 1146-1157 (2006).

[2] L.A. Crum, “Bjerknes forces on bubbles in a stationary sound field”, *The Journal of the Acoustical Society of America*, Vol. 57, No 6, Part 1, 1363-1370 (1975).

[3] X. Xi, F.B. Cegla, R. Mettin, F. Holsteyns and A. Lippert, “Collective bubble dynamics near a surface in a weak acoustic standing wave field”, *Journal of the Acoustical Society of America*, Vol. 132, No 1, 37-47 (2012).

[4] X. Xi, F.B. Cegla, M. Lowe, A. Thiemann, T. Nowak, R. Mettin, F. Holsteyns and A. Lippert, “Study on the bubble transport mechanism in an acoustic standing wave field”, *Ultrasonics*, 51, 1014-1025 (2011).

[5] Z. Douglas, T.R. Boziuk, M.K. Smith and A. Glezer, “Acoustically enhanced boiling heat transfer”, *Physics of Fluids*, Vol. 24, 052105 (2012).

[6] J. S. Sitter, T. J. Snyder, J. N. Chung and P. L. Marston, “Acoustic field interaction with a boiling system under terrestrial gravity and microgravity”, *Journal of the Acoustical Society of America*, Vol. 104, No 5, 2561-2569 (1998).

[7] T.J. Asaki, P.L. Marston and E.H. Trinh, “Shape oscillations of bubbles in water driven by modulated ultrasonic radiation pressure: Observations and detection with scattered laser light”, *Journal of the Acoustical Society of America*, Vol. 23, No 2, 706-713 (1993).

[8] Polytec GmbH, “User Manual Laser Doppler Vibrometer: Controller OFV-3001, Sensor Heads OFV-303”, *Polytec publications*.

[9] Polytec - Advancing Measurements by Light, “Basic Principles of Vibrometry”, *http://www.polytec.com/us/solutions/vibration_measurement/basic_principles_of_vibrometry* [Last visited: 16/02/2014].

[10] B.E. Truax, F.C. Demarest and G.E. Sommargren, “Laser Doppler velocimeter for velocity and length measurements of moving surgaces”, *Applied Optics*, Vol. 23, No 1, 67-73 (1984).

[11] E. Esposito, Department of Mechanics, Polytechnic University of Marche, Ancona, Italy, “Laser Doppler Vibrometry”, *http://www.science4heritage.org/COSTG7/booklet/chapters/ldv.htm* [Last visited: 16/02/2014].

[12] E. Quagliarini, E. Esposito and A. del Conte, “The combined use of IRT and LDV for the investigation of historical thin vaults”, *Journal of Cultural Heritage*, Vol. 14, No 2, 122-128 (2013).

[13] L. Collini and R. Garziera, “A contact-less diagnosis system for frescoes. Part two: Acoustic excitation–acoustic response”, *NDT&E International*, Vol. 56, 76-81 (2013).

[14] P. Shen, K. Flanagan and M. Palmer, “Laser Vibrometer PFC Health Monitoring System”, *Luna Innovations, Blacksburg,* VA 24060 (2011).

[15] Shaker, “Installation and Operating Manual V200 Series Vibrators”, *Manual 892071,* Edition 2, Amendment 12 (1995).

[16] M. O. Culjat, D. Goldenberg, P. Tewari, R. S. Singh, "A Review of Tissue Substitutes for Ultrasound Imaging", *Ultrasound in Medicine & Biology,* Vol. 36, No 6, 861–873 (2010).

[17] L. Jakevičius and A. Demčenko, “Ultrasound attenuation dependence on air temperature in closed chambers”, *ULTRAGARSAS Journal, Ultrasound Institute*, Vol. 63, No.1 (2008).

ANNEX

Displacement maps

Displacement maps in μm at different conditions of the test cell (empty, half and full of water), at different amplitudes (from 1V to 5V) in the face and the back walls of the test cell.

Face – empty – 1V

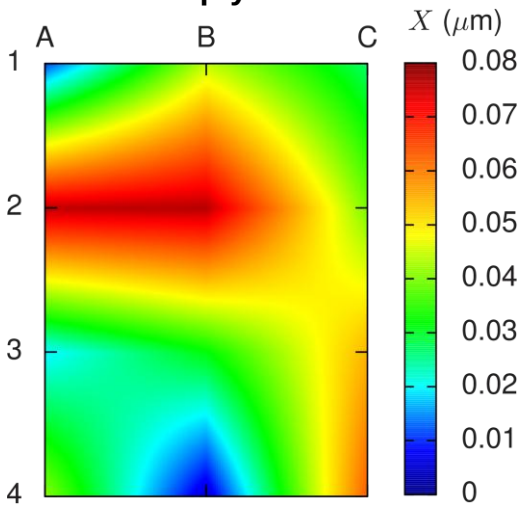

Back – empty – 1V

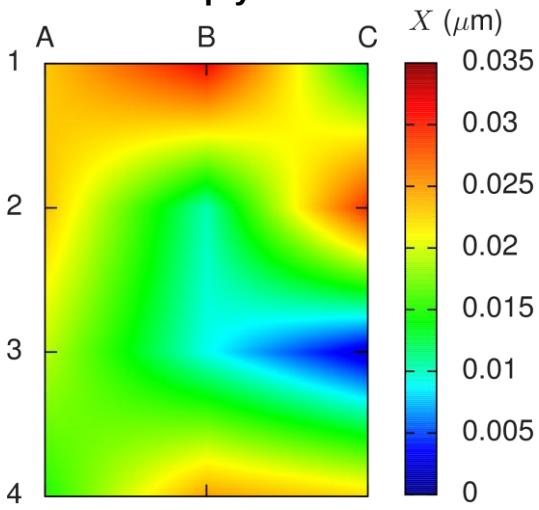

Face – half – 1V

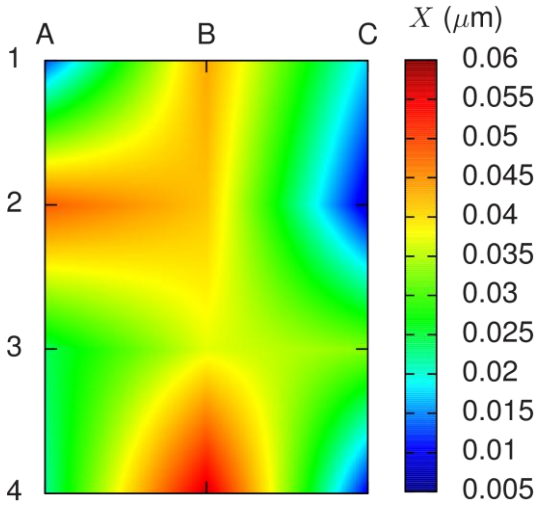

Back – half – 1V

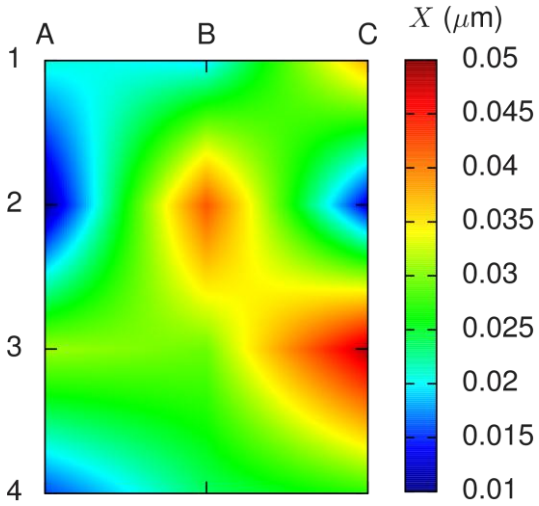

Face – full – 1V

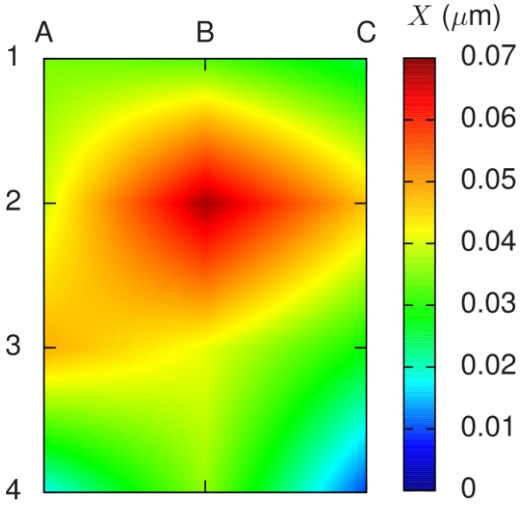

Back – full – 1V

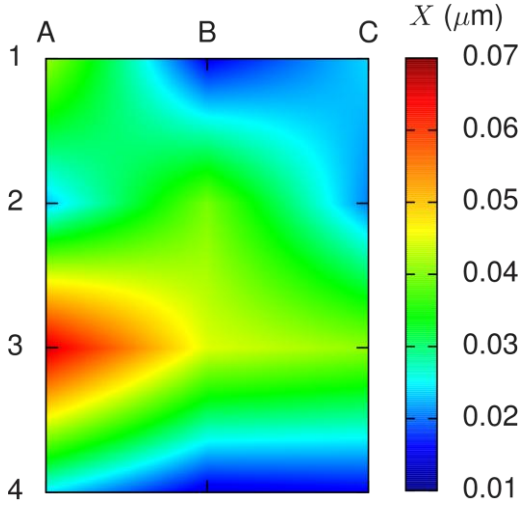

Face – empty – 2V

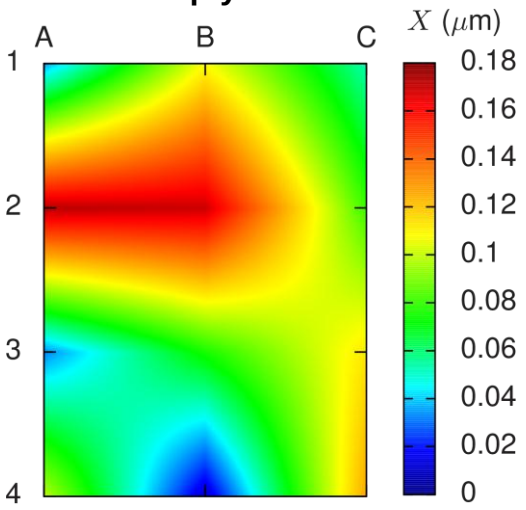

Back – empty – 2V

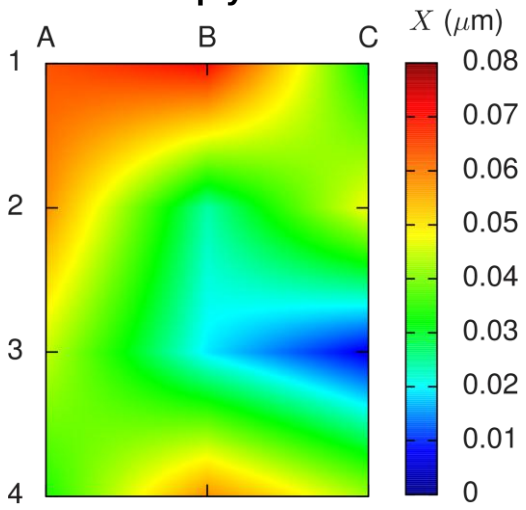

Face – half – 2V

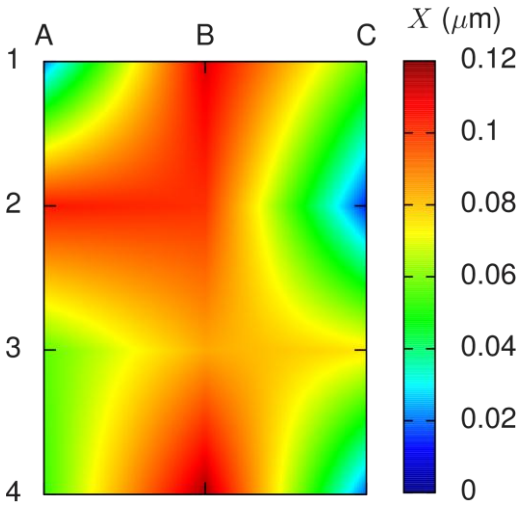

Back – half – 2V

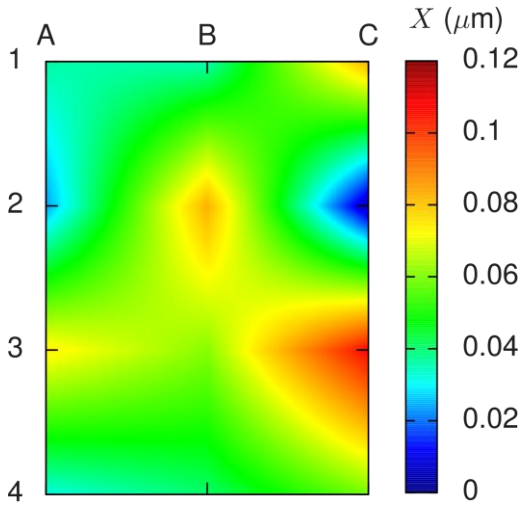

Face – full – 2V

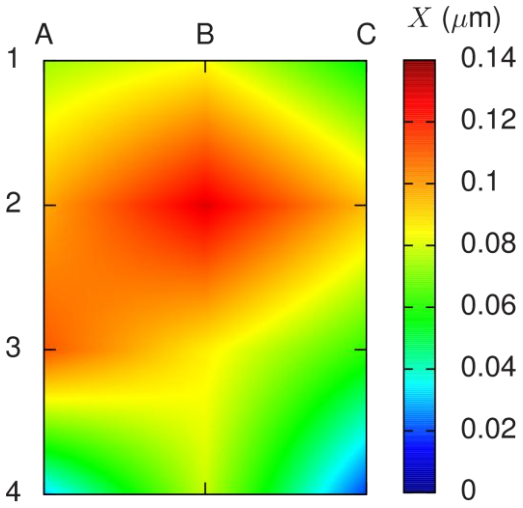

Back – full – 2V

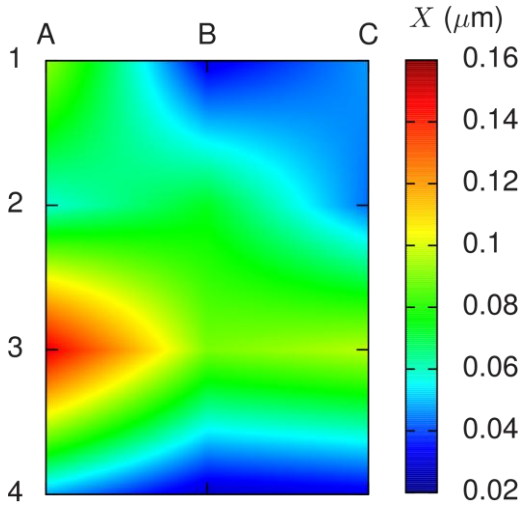

Face – empty – 3V

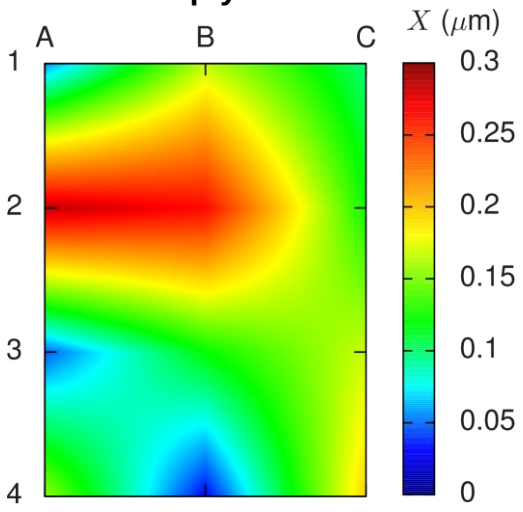

Back – empty – 3V

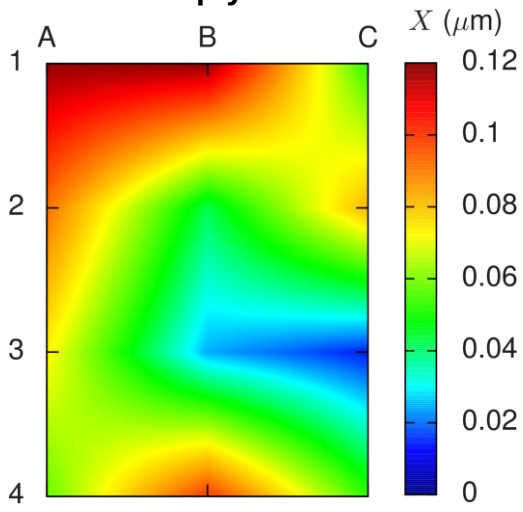

Face – half – 3V

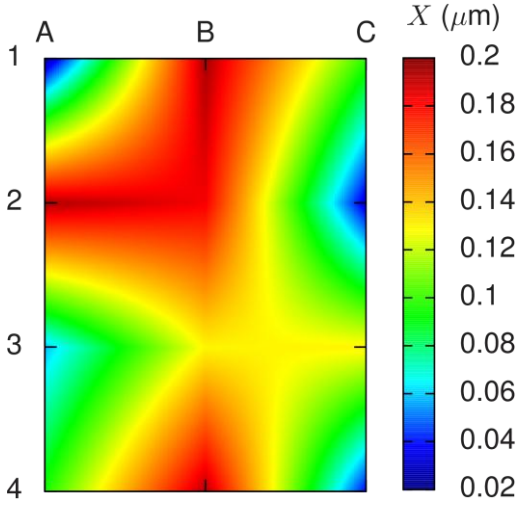

Back – half – 3V

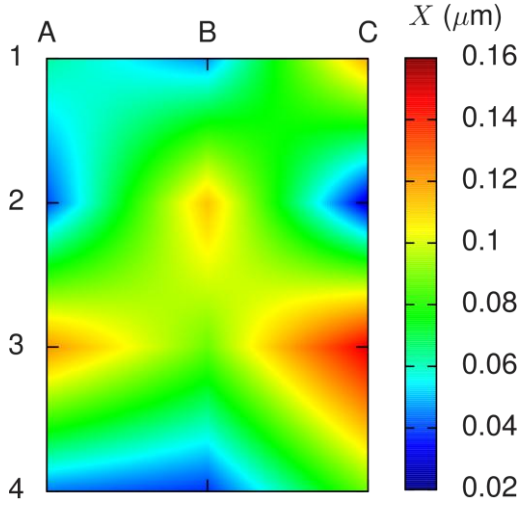

Face – full – 3V

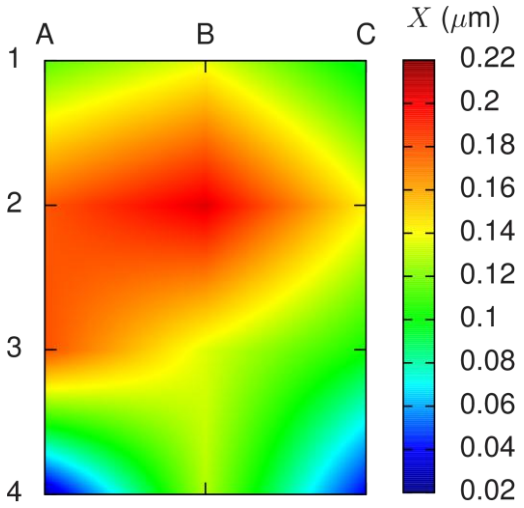

Back – full – 3V

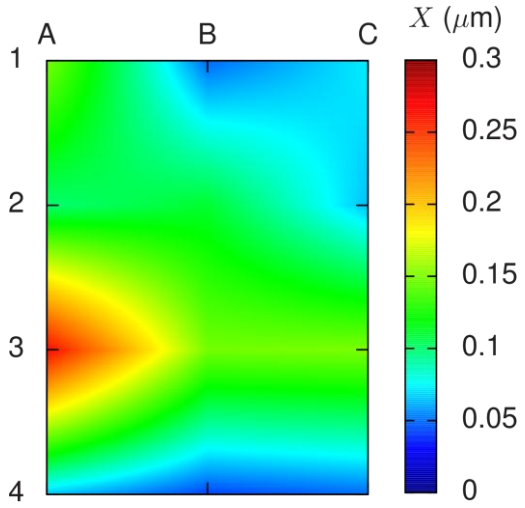

Face – empty – 4V

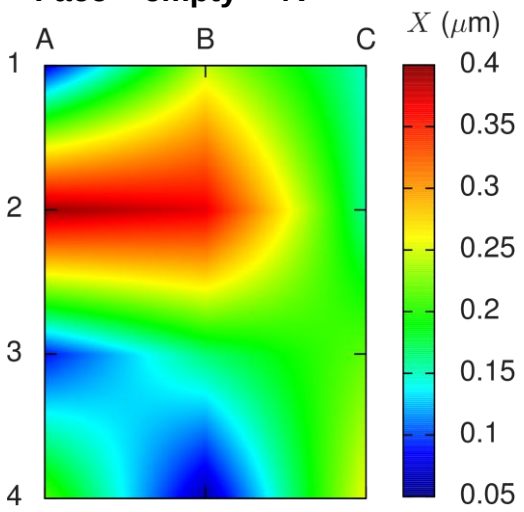

Back – empty – 4V

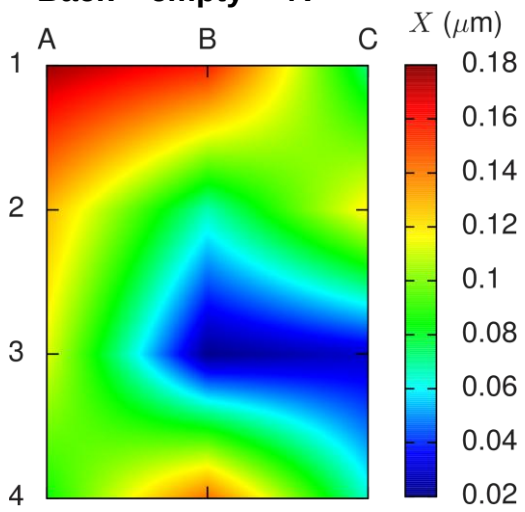

Face – half – 4V

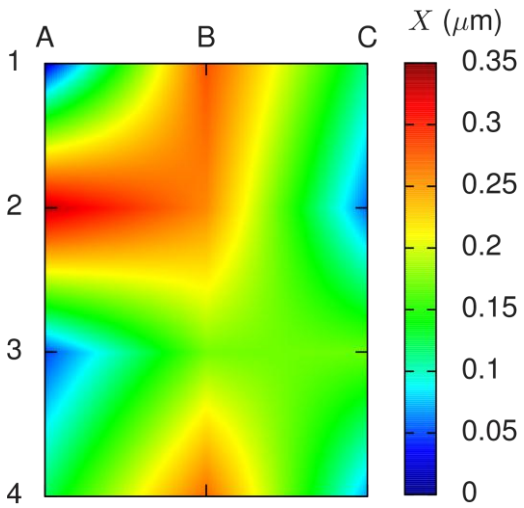

Back – half – 4V

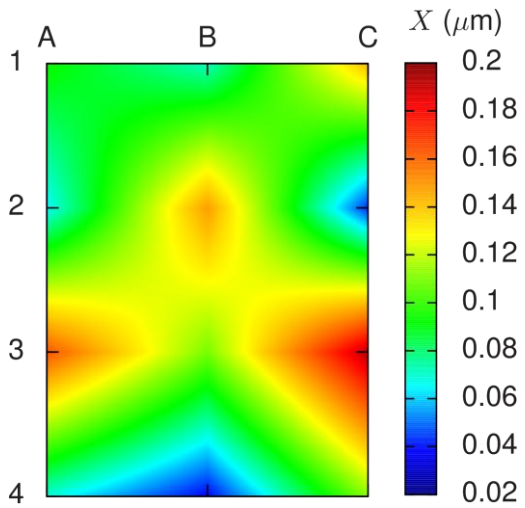

Face – full – 4V

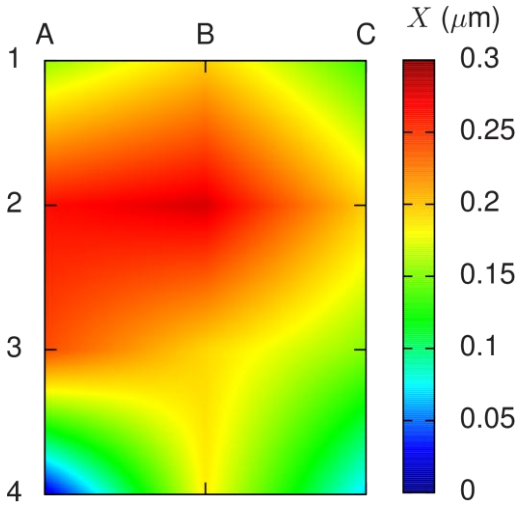

Back – full – 4V

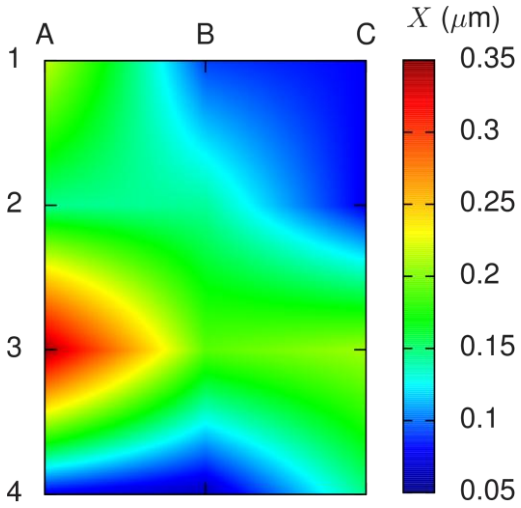

Face – empty – 5V

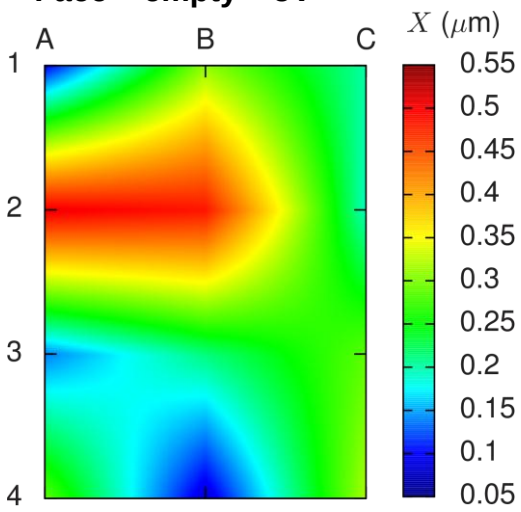

Back – empty – 5V

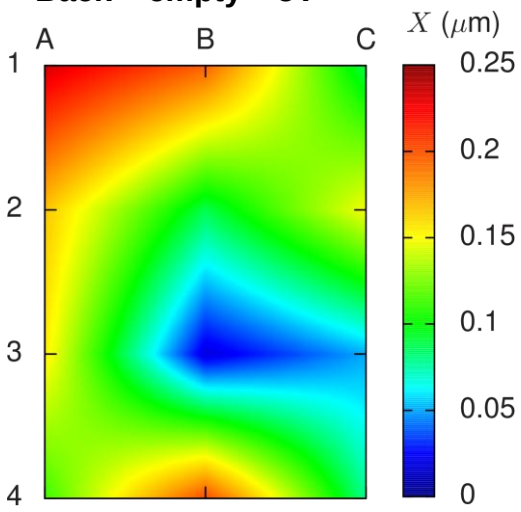

Face – half – 5V

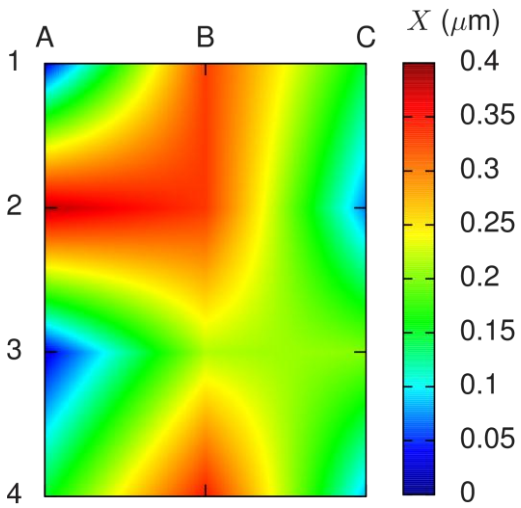

Back – half – 5V

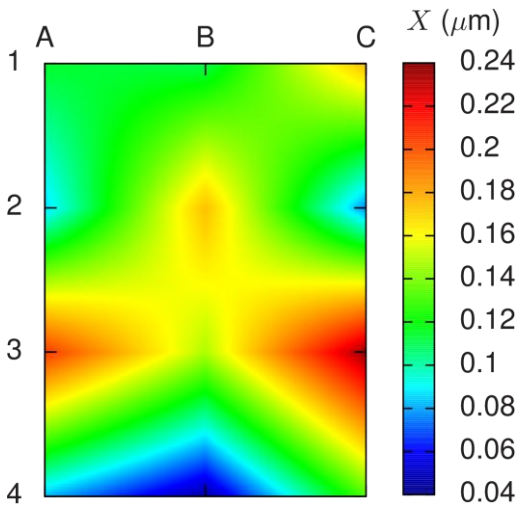

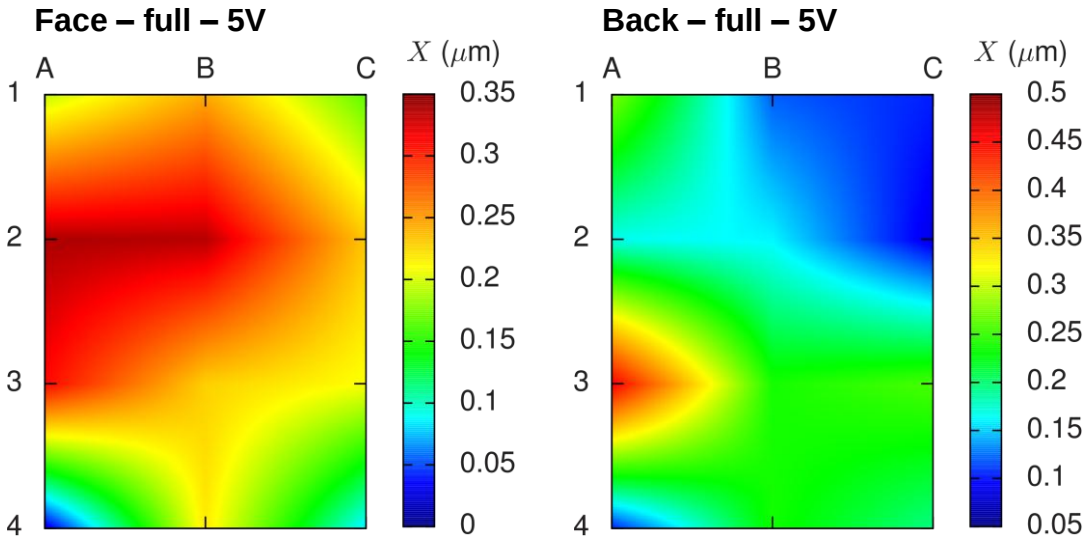
Face – full – 5V
A
B
C
1
2
3
4
X (μm)
0.35
0.3
0.25
0.2
0.15
0.1
0.05
0
Back – full – 5V
A
B
C
1
2
3
4
X (μm)
0.5
0.45
0.4
0.35
0.3
0.25
0.2
0.15
0.1
0.05

Frequency evolution at 30-60kHz region in B3 cell

Displacement in μm as a function of the frequency applied in the piezoelectric from 30 kHz to 60 kHz at different conditions (empty, half and full of water), at different amplitudes (from 1V to 6V) in the face and the back walls of the B3 cell from the test cell.

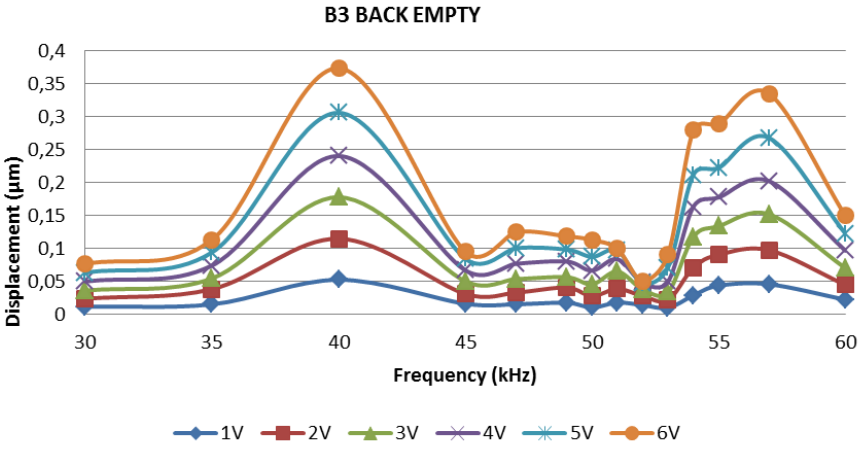

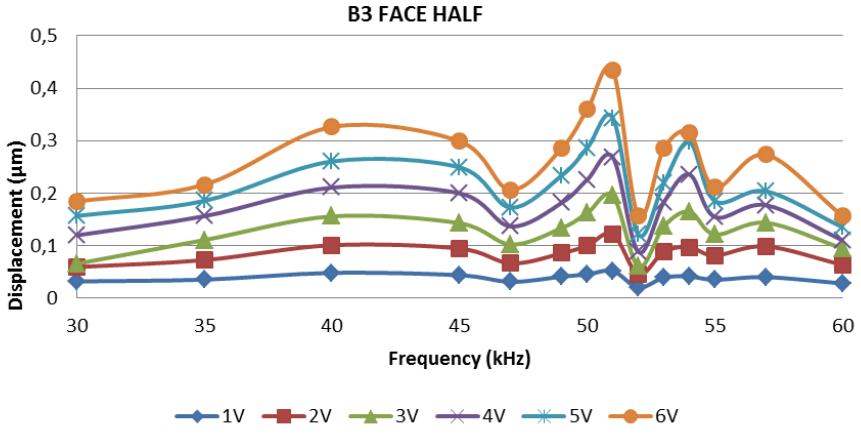

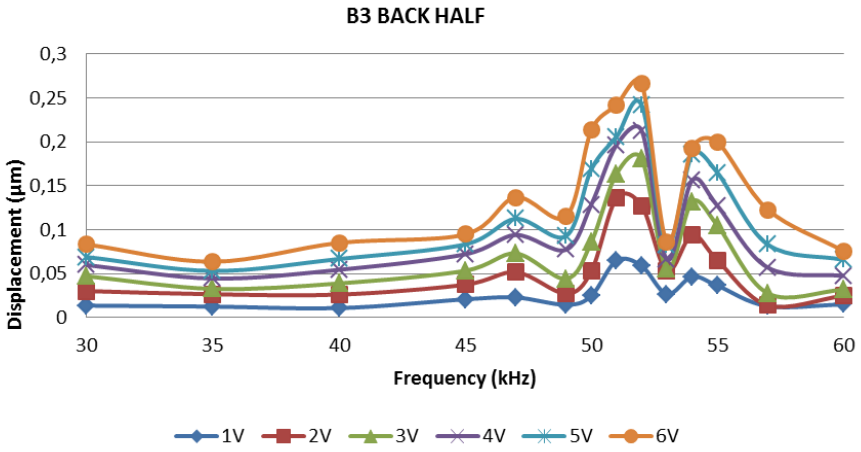
B3 BACK HALF
Displacement (µm)
0,3
0,25
0,2
0,15
0,1
0,05
0
30
35
40
45
50
55
60
Frequency (kHz)
1V
2V
3V
4V
5V
6V

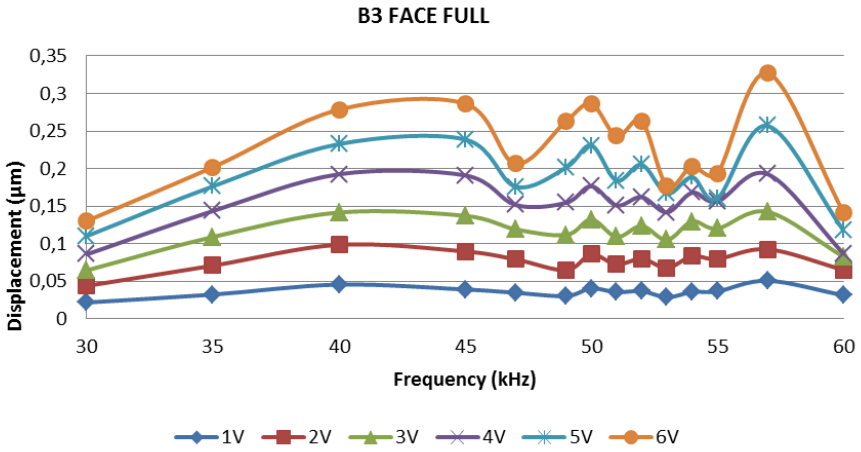
B3 FACE FULL
Displacement (µm)
0,35
0,3
0,25
0,2
0,15
0,1
0,05
0
30
35
40
45
50
55
60
Frequency (kHz)
1V
2V
3V
4V
5V
6V

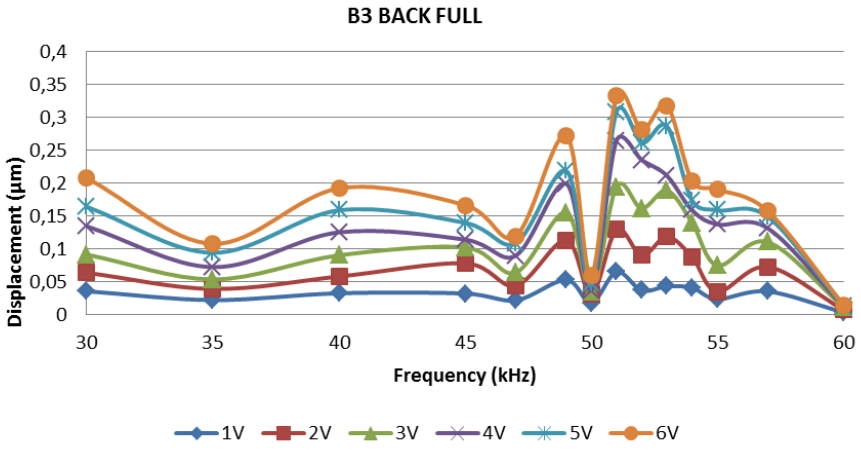
B3 BACK FULL
Displacement (µm)
0,4
0,35
0,3
0,25
0,2
0,15
0,1
0,05
0
30
35
40
45
50
55
60
Frequency (kHz)
1V
2V
3V
4V
5V
6V

Frequency evolution in C1/A1 cell

Displacement in μm as a function of the frequency applied in the piezoelectric from 5 kHz to 200 kHz at different conditions (empty, half and full of water), at different amplitudes (from 1V to 6V) in the face and the back walls of the C1/A1 cell from the test cell.

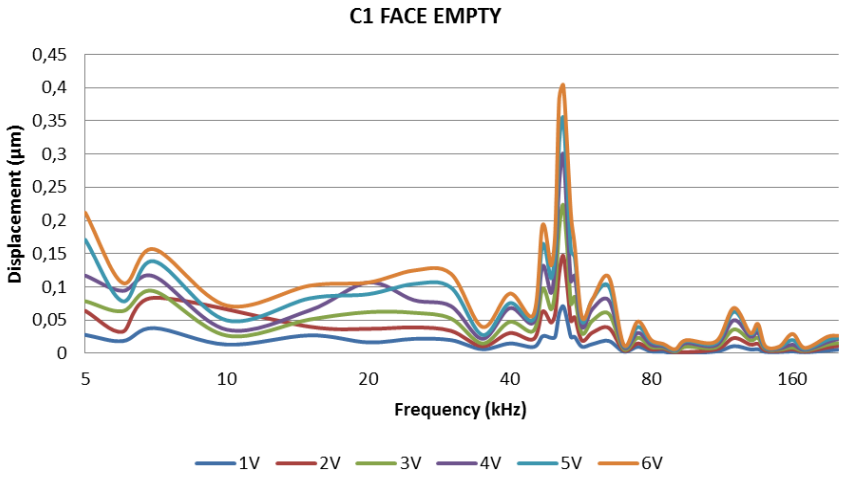

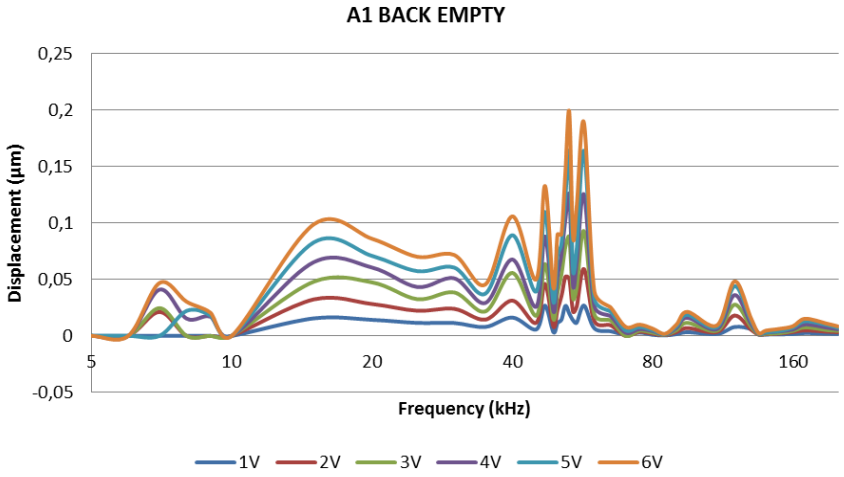

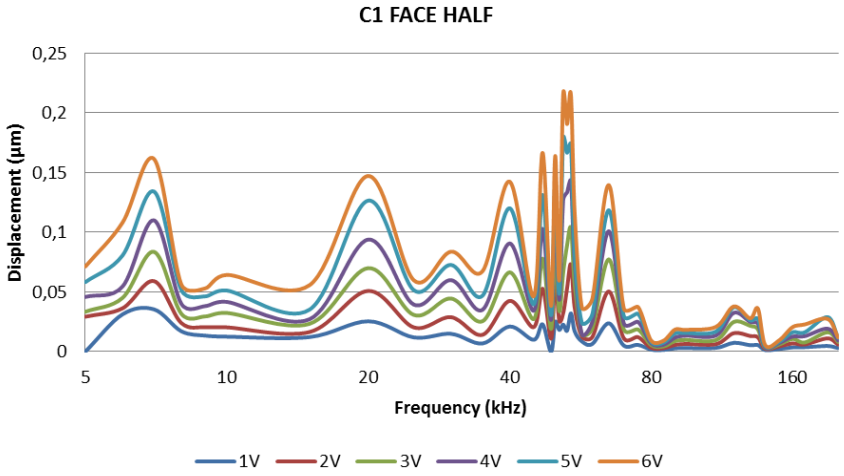

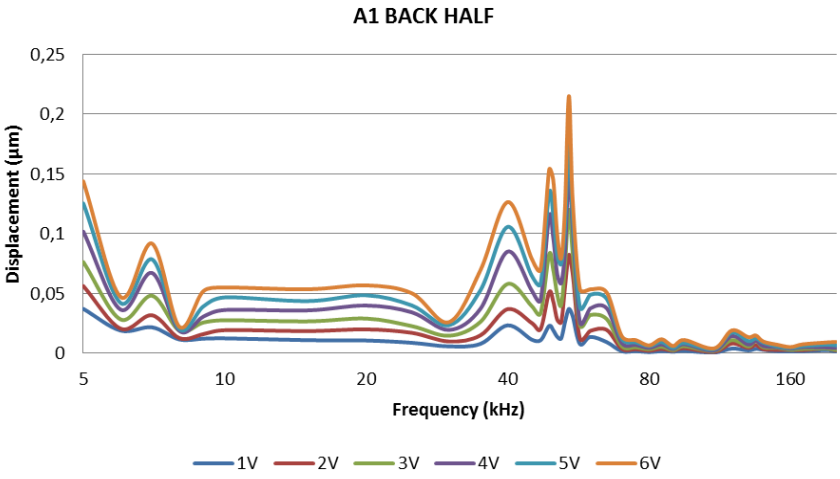
A1 BACK HALF
Displacement (µm)
0,25
0,2
0,15
0,1
0,05
0
5
10
20
40
80
160
Frequency (kHz)
1V
2V
3V
4V
5V
6V

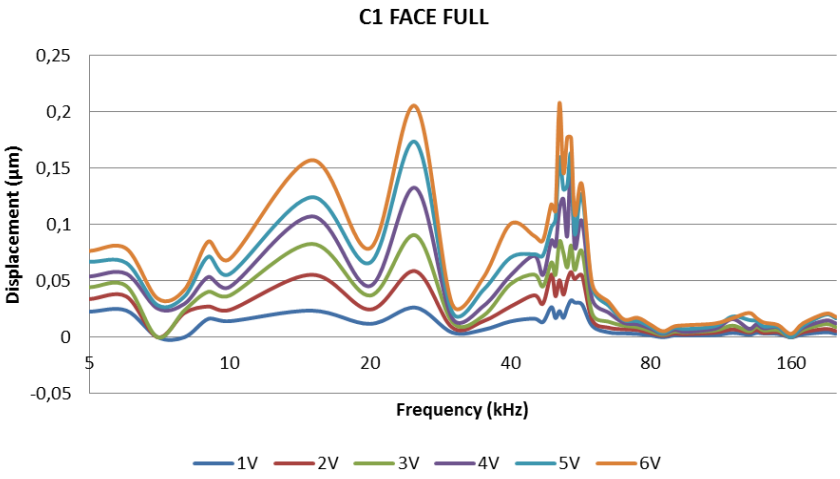
C1 FACE FULL
Displacement (µm)
0,25
0,2
0,15
0,1
0,05
0
-0,05
5
10
20
40
80
160
Frequency (kHz)
1V
2V
3V
4V
5V
6V

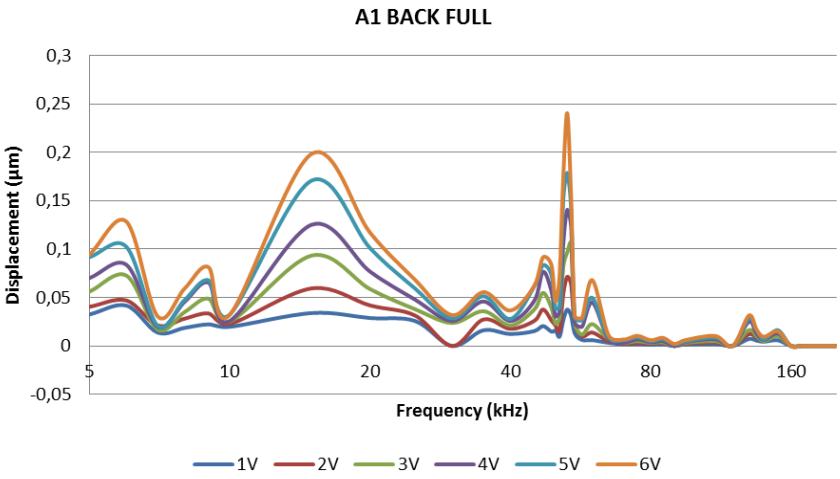
A1 BACK FULL
Displacement (µm)
0,3
0,25
0,2
0,15
0,1
0,05
0
-0,05
5
10
20
40
80
160
Frequency (kHz)
1V
2V
3V
4V
5V
6V

Frequency evolution at 30-60kHz region in C1/A1 cell

Displacement in μm as a function of the frequency applied in the piezoelectric from 30 kHz to 60 kHz at different conditions (empty, half and full of water), at different amplitudes (from 1V to 6V) in the face and the back walls of the C1/A1 cell from the test cell.

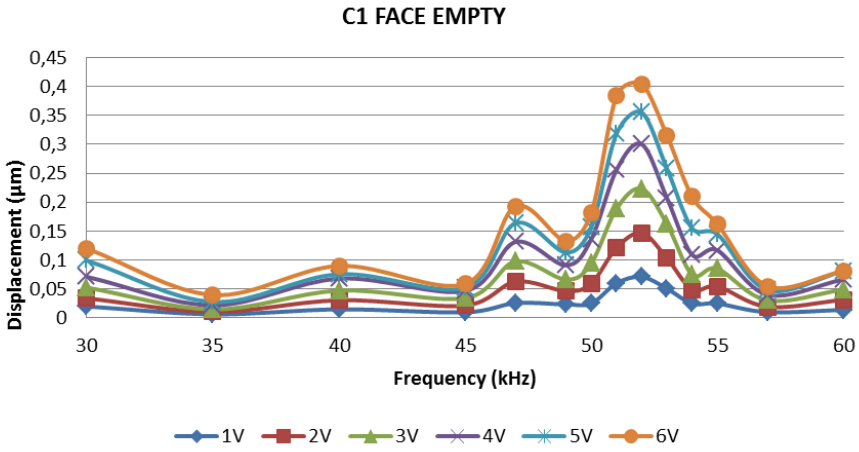

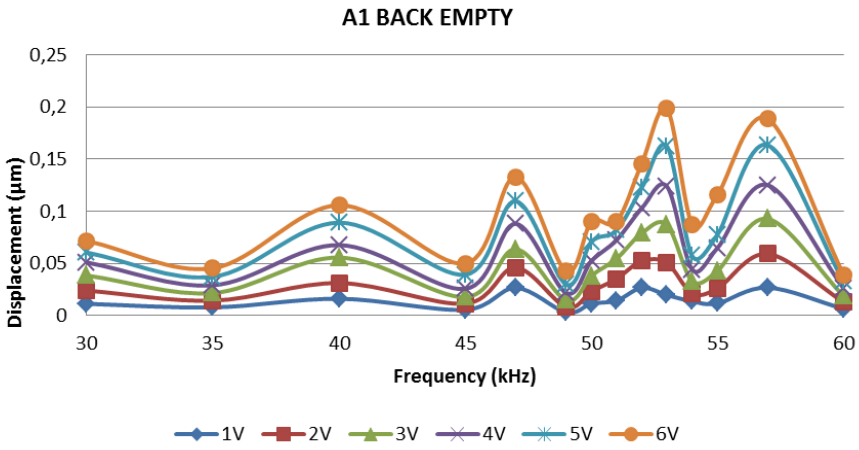

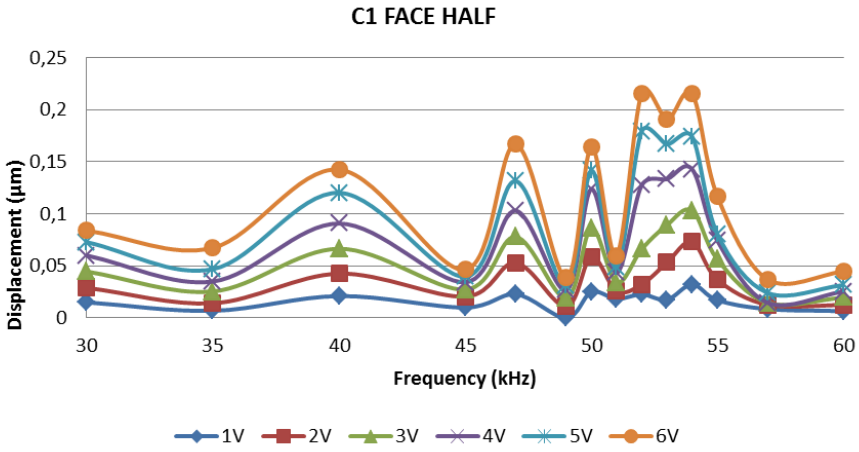

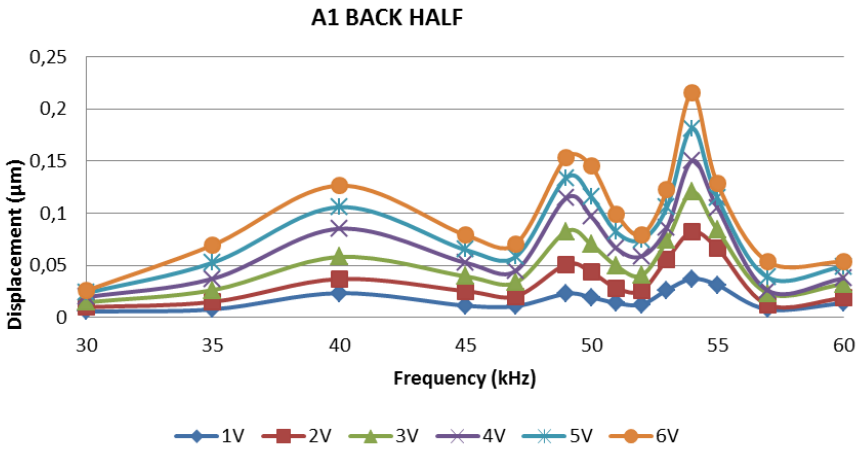
A1 BACK HALF
Displacement (µm)
0,25
0,2
0,15
0,1
0,05
0
30
35
40
45
50
55
60
Frequency (kHz)
1V
2V
3V
4V
5V
6V

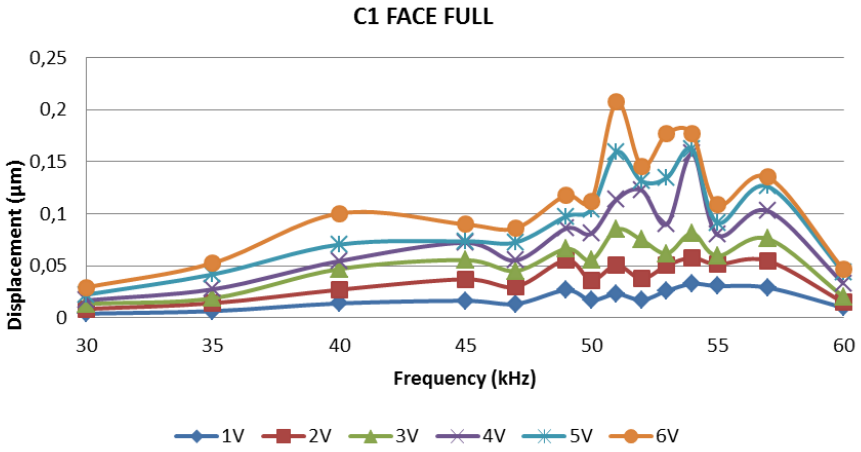
C1 FACE FULL
Displacement (µm)
0,25
0,2
0,15
0,1
0,05
0
30
35
40
45
50
55
60
Frequency (kHz)
1V
2V
3V
4V
5V
6V

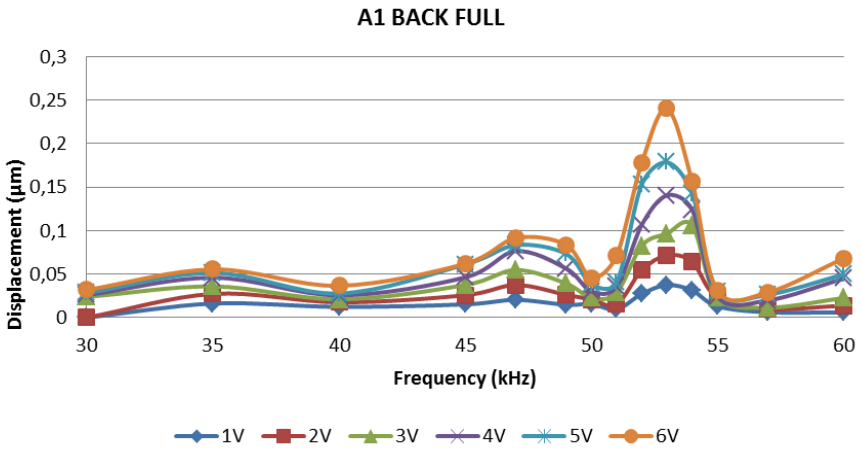
A1 BACK FULL
Displacement (µm)
0,3
0,25
0,2
0,15
0,1
0,05
0
30
35
40
45
50
55
60
Frequency (kHz)
1V
2V
3V
4V
5V
6V